ISTANBUL TECHNICAL UNIVERSITY ★ GRADUATE SCHOOL OF SCIENCE
ENGINEERING AND TECHNOLOGY

MACHINE LEARNING AIDED KIDNEY STONE CLASSIFICATION WITH ELECTROMAGNETIC PROPERTIES

M.Sc. THESIS

Banu SAÇLI

Department of Electronics and Communication Engineering

Biomedical Engineering Programme

JUNE 2018

ISTANBUL TECHNICAL UNIVERSITY ★ GRADUATE SCHOOL OF SCIENCE ENGINEERING AND TECHNOLOGY

MACHINE LEARNING AIDED KIDNEY STONE CLASSIFICATION WITH ELECTROMAGNETIC PROPERTIES

M.Sc. THESIS

Banu SAÇLI
(504161411)

Department of Electronics and Communication Engineering

Biomedical Engineering Programme

Thesis Advisor: Assoc. Prof. Mehmet ÇAYÖREN

JUNE 2018

İSTANBUL TEKNİK ÜNİVERSİTESİ ★ FEN BİLİMLERİ ENSTİTÜSÜ

MAKİNE ÖĞRENMESİ YARDIMIYLA BÖBREK TAŞLARININ ELEKTROMANYETİK ÖZELLİKLERİNİN SINIFLANDIRILMASI

YÜKSEK LİSANS TEZİ

Banu SAÇLI
(504161411)

Elektronik Haberleşme Mühendisliği Anabilim Dalı

Biyomedikal Mühendisliği Programı

Tez Danışmanı: Assoc. Prof. Mehmet ÇAYÖREN

HAZİRAN 2018

Banu SAÇLI, a M.Sc. student of ITU Graduate School of Science Engineering and Technology 504161411 successfully defended the thesis entitled "MACHINE LEARNING AIDED KIDNEY STONE CLASSIFICATION WITH ELECTROMAGNETIC PROPERTIES", which he/she prepared after fulfilling the requirements specified in the associated legislations, before the jury whose signatures are below.

Thesis Advisor :	**Assoc. Prof. Mehmet ÇAYÖREN** Istanbul Technical University	....
Jury Members :	**Asst. Prof. Tuba YILMAZ ABDOLSAHEB** Istanbul Technical University	....
	Asst. Prof. Evrim TETİK Istanbul Aydın University	....
		....

Date of Submission : **4 May 2018**
Date of Defense : **7 June 2018**

To my parents,

FOREWORD

I specifically would like to thank my supervisor, Assoc. Prof. Mehmet ÇAYÖREN for their excellent guidance and support during my research. I would also like to thank Asst. Prof. Tuba YILMAZ ABDOLSAHEB and Prof. İbrahim AKDUMAN for their valuable advices throughout this study. I would also like to thank Prof. Bülent ÖNAL for allowing us to get kidney stones.

I also wish to thank my friends Gökhan CANSIZ and Sulayman JOOF for their help during dielectric measurements of kidney stones. I would not have been able to conduct this study without their cooperation.

I am grateful to Melih BİLMEZ for his constant love, support and patience. He did not only motivate me whenever I lost my interest, but he also discuss ideas about my research. I cannot express how lucky I am for having a companion like him.

Finally, despite it is hard to express my deepest gratitude to my parents and my sisters, I would like to thank them for their love and sacrifices.

June 2018 Banu SAÇLI

TABLE OF CONTENTS

Page

ABBREVIATIONS

ANN	: Artificial Neural Network
KNN	: k-Nearest Neighborhood
CT	: Computed Tomography
KUB	: Kidneys, Ureters and Bladder
IVP	: Intravenous Pyelogram
US	: Ultrasonography
MRI	: Magnetic Resonance Imaging
ESWL	: Extracorporeal Shockwave Therapy
PCNL	: Percutaneous Nephrolithotomy
SEM	: Scanning Electron Microscopy
IR	: Infrared Radiation
XRD	: X-Ray Powder Diffraction
GNR	: Generalized Newton-Raphson
tp	: True Positive
fp	: False Positive
fn	: False Negative
tn	: True Negative

SYMBOLS

E	: Electric Field
H	: Magnetic Field
D	: Dielectric Displacement
B	: Magnetic Induction
j	: Current Density
$\boldsymbol{\rho}_e$	: Charge Density
$\boldsymbol{\varepsilon}$	: Absolute Permittivity
$\boldsymbol{\varepsilon}^*$	: Relative Permittivity
$\boldsymbol{\varepsilon}_0$	: Permittivity of Free Space
$\boldsymbol{\varepsilon}'$	: Dielectric Constant
$\boldsymbol{\varepsilon}''$	: Dielectric Loss Factor
$\boldsymbol{\sigma}$	: Electrical Conductivity
w	: Angular Frequency
$\boldsymbol{\varepsilon}_\infty$	: Infinite Frequency Dielectric Constant
$\boldsymbol{\varepsilon}_s$	: Static Dielectric Constant
$\boldsymbol{\tau}$	: Relaxation Time
Y	: Admittance
$\boldsymbol{\Gamma}$	: Reflection Coefficient
W	: Weight at Artificial Neuron
$\boldsymbol{\delta}$	: Error Gradient
$\boldsymbol{\eta}$	: Learning Rate of Neural Network

LIST OF TABLES

LIST OF FIGURES

Page

MACHINE LEARNING AIDED KIDNEY STONE CLASSIFICATION WITH ELECTROMAGNETIC PROPERTIES

SUMMARY

Electromagnetic waves with microwave frequencies have been widely used in medical field for diagnostic and therapeutic purposes. The reasons why microwaves have been preferred are mainly its non-ionizing nature and its ability to penetrate matter. Physiological effect on biological tissues also enables to use for treatment of diseases. Moreover, the difference in electromagnetic properties of distinct biological material enables diagnostic usage. In this study, the determination of kidney stone types was aimed by making use of the dielectric discrepancy between stone types.

It is known from statical information that the recurrence rate of kidney stone disease is very high. For this reason, it is important to learn why the body forms kidney stones in order to determine necessary precautions to prevent recurrence. The tools utilized for determination of the reasons for stone formation are blood test, urine test and tools used for urinary stone analysis. To this end, this study focused on development of an innovative method for urinary stone analysis.

When dielectric property measurements of three common types of kidney stone were carried out, it is realized that it is possible to distinguish kidney stones with machine learning algorithms and the help of these features. Dielectric constant and dielectric loss values of each stone were measured over the frequency range of 500 MHz – 6 GHz with 100 MHz intervals. Then, Cole-Cole parameters of each stone were calculated with generalized Newton-Raphson method from measured dielectric constant and dielectric loss values instead of directly use of them. Thus, the input size of machine learning algorithm was reduced with successful Cole-Cole fitting.

After dielectric property measurement and Cole-Cole fitting, classification of the stones were completed with an artificial neural network and k-nearest neighborhood algorithm. Obtained classification of two algorithm were evaluated with some performance measures which are accuracy, sensitivity, specificity, precision, recall and F1 score. It can obviously be seen from these measures that both of two classifier are quite successful in determination of kidney stone types.

MAKİNE ÖĞRENMESİ YARDIMIYLA BÖBREK TAŞLARININ ELEKTROMANYETİK ÖZELLİKLERİNİN SINIFLANDIRILMASI

ÖZET

Mikrodalga frekansında elektromanyetik dalgalar iyonlaşmaya sebep olmadan maddeye nüfus edebildiğinden dolayımedikal alanda güvenle kullanılabileceği düşünülmektedir. Hastalıkların teşhis ve tedavisinde mikrodalga kullanımına yönelik çalışmalar hızlıbir şekilde yürütülmektedir. Dokulara mikrodalga uygulandığında bölgede görülen ısıartışıgibi fizyolojik etkiler, bu etkilerin pozitif yönde kullanılarak bazıhastalıkların tedavisinde kullanılabileceği düşüncesini ortaya çıkarmıştır. Kanser tedavisinde kullanılan mikrodalga hipertermi bu düşüncenin bir ürünüdür. Ayrıca, biyolojik doku ve malzemelerin dielektrik özelliklerinin farklıolmasıve özellikle hastalık söz konusu olduğunda bu özelliklerin değişmesi teşhis amaçlıkullanımınımümkün kılmıştır.

Bugüne kadar yapılan mikrodalga ile teşhis sistemleri geliştirmeye yönelik çalışmalarıbasitçe ele alacak olursak, ilgili bölgedeki dokulara mikrodalga gönderilmesi ve bu bölgeden yansıyan dalganın algılanmasıprensibine dayandığınısöyleyebiliriz. Görüntülenen bölgedeki dokuların farklıolması, bu dokulardan yansıyan dalganın, dolayısıyla hesaplanan dielektrik özelliklerinin farklıolmasına sebep olur. Çalışmaların birçoğunda, bu farklılıktan faydalanılarak ilgili bölgenin dielektrik ve iletkenlik haritalarıoluşturulmaktadır ve bu haritalar teşhis amaçlıkullanılabilmektedir. Ayrıca, literatürdeki bu çalışmalar incelendiğinde özellikle kanser türlerinin teşhisine odaklanıldığıve başarılısonuçlar elde edildiği görülmektedir. Bu da kanser dışındaki hastalıkların teşhisine yönelik çalışmalara umut olmuştur. Bu çalışmada da farklıtüre ait böbrek taşlarının dielektrik özelliklerindeki farklılıktan faydalanılarak türlerinin belirlenmesinin mümkün olup olmadığısorusuna cevap aranmıştır.

Boşaltım sisteminin vücudun sıvı, pH ve kan basıncıdengesini sağlamasıve zehirli atıklarıvücuttan uzaklaştırmasıgibi hayati önem taşıyan fonksiyonlarıvardır. Bu nedenle, boşaltım sistemi organlarından birinde herhangi bir problem olduğunda hastanın hayatıoldukça zorlaşmaktadır. Böbrek taşıhastalığıbu problemlerden birisidir ve hastaların yaşam kalitesini oldukça düşürmektedir. Hastalığın Türkiye'de görülme sıklığı%11 iken tekrar etme sıklığı %80'dir. Vücut içindeki böbrek taşlarıbilgisayarlıtomografi, X-ray, ultrason, manyetik rezonans gibi araçlarla teşhis edilir. Ardından hekim tarafından uygun görülen yöntemlerden biriyle vücuttan uzaklaştırılır. Vücudun böbrek taşınıneden oluşturduğunu anlamak tekrar oluşmamasıiçin alınacak önlemleri belirlemekte oldukça önemlidir. Bu amaçla hastaya kan ve 24-saatlik idrar tahlilleri yapılmaktadır. Ayrıca, çıkarılan böbrek taşının analizi yapılarak çeşidinin belirlenmesi de önemli bir rol oynamaktadır. Bu çalışmayla böbrek taşıtürünün belirlenmesinde mevcut metotlara mikrodalga frekansında elektromanyetik dalgalardan faydalanan yeni bir alternatif geliştirmek amaçlanmıştır.

İlk olarak üç sınıfa ait 105 adet böbrek taşının açık uçlu koaksiyel sonda ile dielektrik ölçümlerinin yaılabilmesi için hazırlanmıştır.Taş yüzeyleri mümk ün

oldugunca pürüzsüz hale getirilmiş ve hava boşlugu kalmayacak şekilde probla teması saglanmıştır. Daha sonra mevcut deney düzenegi ile böbrek taşlarının dielektrik ölçümleri gerçekleştirilmiştir. Deney düzenegi istenilen frekansta sinyal üreten ve yansıyan sinyali algılayan bir ag analizörü; bu sinyali maddeye, maddeden yansıyan sinyali de ag analizörüne ileten bir prob, ölçülen S_{11} parametresinden dielektrik sabiti ve dielektrik kaybınıhesaplayan bir yazılım ve bu yazılımın kullanıldıgıbir harici bilgisayardan oluşmaktadır. Ag analizörü, 500 MHz – 6 GHz aralığında 100 MHz aralıklarla sinyal üretecek şekilde hazırlanmış, ve hava, proba özel iletken bir malzeme ve deiyonize su ile kalibrasyonu yapılmıştır.

Taşların törpülenme işlemini ve kalibrasyon sürecini tamamladıktan sonra ayarlanan frekansta böbrek Taşlarının dielektrik özellik ölççümü yapılmıştır. Ölçümler her bir taş için beş kere tekrar edilerek alınan sonuçların medyanları, taşın dielektrik özellikleri olarak kabul edilmiştir. Böylece ölçüm hataları en aza indirilmeye çalışılmıştır. Sonuç olarak toplam 56 noktada, her bir taşın dielektrik sabiti ve dielektrik kaybı, dolayısıyla kompleks permittivitisi elde edilmiştir. Ardından bu değerler Cole-Cole denkleminde yerine koyularak, her bir taş için 5 bilinmeyeni olan ve 56 adet eşitlikten oluşan bir denklem sistemi elde edilmiştir. Bu 5 bilinmeyen, Cole-Cole parametresi olarak adlandırılan statik dielektrik, yüksek frekanslarda dielektrik, rahatlama frekansı, dagılım degışkeni ve statik elektriksel iletkenliktir.

Bu denklem sistemi genelleştirilmiş Newton-Raphson yönteminden faydalanılarak çözülmüştür. Bu yöntem denklemin kısmi türevlerinden faydalanarak çözülmesine dayanan iterativ bir nümerik metottur. Bu yöntemle çözüm yapabilmek için önce Cole-Cole parametrelerine başlangıç degerleri atanmış ve daha sonra bu degerler hesaplanan hataya göre iterativ olarak güncellenmiştir. Sonuç olarak her bir taşın Cole-Cole parametresi bulunmuştur. Ayrıca, bulunan bu parametreler yine aynıdenklemde yerine koyularak dielektrik sabiti ve dielektrik kaybıhesaplanmıştır. Hesaplanan bu değerler ölçülen değerlerle aynıeksende çizdirildiğinde ölçülen değerlere oldukça iyi oturduğu görülmektedir. Bu sürecin sonunda, 105 taş için beşer adet Cole-Cole parametresi hesaplanmış olmuştur.

Her bir taşın Cole-Cole parametreleri hesaplandıktan sonra makine öğrenmesi algoritmaları ile sınıflandırılması yapılmıştır. Cole-Cole parametreleri algoritmaların giriş degerlerini oluştururken, böbrek taşı sınıflarını içeren nümerik bir vektör de çıkış degerlerini oluşturmaktadır. Öncelikle bu giriş ve çıkış degerleri, egitim süresini kısaltmak amacıyla (-1, 1) aralıgında normalize edilmiştir. Normalizasyon sonrasında, böbrek taşları k-sayısı kadar çapraz dogrulama yöntemiyle egitim ve test kümelerine ayrılmıştır. Bu çalışmada k sayısı 5 olarak seçilmiştir.

Makine ögrenmesi algoritması olarak ilk önce bir gizli katmandan oluşan üş katmanlı bir yapay sinir agı tasarlanmıştır. 5 adet giriş ve 1 adet çıkış oldugundan dolayı giriş ve çıkış katmanlarındaki nöron sayısı sırasıyla beš ve bir olarak ayarlanmıştır. Gizli katmandaki nöron sayısı ise on beş olarak seçilmiştir. Gizli katmanın aktivasyon fonksiyonu sigmoid fonksiyon olarak belirlenirken, çıkış katmanında lineer fonksiyon tercih edilmiştir. Ag yapısı oluşturulduktan sonra, egitim kümesindeki verilerle dereceli azalan fonksiyon kullanılarak agın egitimi tamamlanmıştır. Daha sonra test kümesindeki verilerin sınıfları tahmin edilerek agın performans ölçütleri hesaplanmıştır.

Kullanılan diger bir makine ögrenmesi algoritması ise k-en yakın komşuluk algoritmasıdır. Bu non-parametrik algoritma, test kümesindeki verilerin her birine en yakın k sayıda egitim verisinin sonucuna bakılarak test verilerinin sonuçlarının belirlenmesi mantıgına dayanır. Bu çalışmada da test amaçlı kullanılan taşların sınıfı, kendılerine en yakın 5 adet egitim amaçlı kullanılan taşın sınıfına göre belirlenmiştir. Uzaklık ölçütü olarak öklit bagıntısı kullanılmıştır. Test kümesindeki tüm taşların sınıfı tahmin edildikten sonra bu algoritma için de performans ölçütleri ayrıca hesaplanmıştır.

Makine ögrenmesi algoritmalarının başarısını hesaplamakta kullanılan başlıca performans ölçütleri dogruluk, duyarlılık, belirleyicilik, kesinlik ve F-ölçütüdür. Bu ölçütleri belirlemek için karışıklık matrisinden faydalanılır. Bu matrisin elemanları sırasıyla gerçek pozitif, sahte pozitif, sahte negatif ve gerçek negatiftir. Her iki algoritmanın sınıflandırma sonuçlarına göre karışıklık matrisleri oluşturulmuş ve performans ölçütleri hesaplanmıştır. Sonuç olarak yapay sinir agı algoritması için tüm performans ölçütlerinin %97'nin üzerinde oldugu görülmüştür. Aynı performansölçütleri, k en yakın komşuluk algoritması için %99'un üzerindedir.

1. INTRODUCTION

The interaction of electromagnetic fields and human body has been studied for a long time in order to make use of electromagnetism technology in diagnosis and therapeutic systems. The nature of electromagnetic fields, that is non-ionizing and has an ability to penetrate matter, enables the use in medical field. The difference in electromagnetic properties of different biological tissues in dependence of their health conditions also makes it possible to use for diagnosis of diseases. Physiological effect of electromagnetic fields at microwave frequencies on tissues provokes the use for treatment of diseases. All these features of electromagnetic interaction give impetus to use electromagnetism in development of new diagnostic and treatment methodologies that do not hurt the patient, save time and minimize the risk of infection. It can also cooperate with current systems to improve their quality and efficiency.

The use of electromagnetic technology in the diagnostic field can be for imaging of interested region. In this frame, measured data is processed and converted into dielectric and conductivity maps of the region. An example of such electromagnetic diagnostic systems can be microwave tomography for early detection of breast cancer [1]. In this system, tumor can be identified, and location and size of the tumor can be got from contrast, dielectric and conductivity maps. Thanks to use of non-ionizing radiation and higher sensitivity in younger women, this microwave tomography system can be an alternative to mammography.

Measured data from the region of interest after applied electromagnetic waves at microwave frequencies can be used for diagnosis without conversion to image. A decision about the pathological status and type of tissues or biological materials can be made with classification methods such as machine learning algorithms [2]. Similar studies for certain diseases have been carried out at different research centers in order to obtain diagnostic information based on the use of electromagnetic fields at microwave frequencies. It is aimed in all these studies to provide more accurate, less painful and early diagnosis of some diseases.

An example for therapeutic application is microwave hyperthermia [3]. In this methodology, interested region is heated with microwave energy and apoptosis of diseased cells is supported. The propagation of the electromagnetic signal and its interaction with biological structures are vital for the efficient treatment. Furthermore, it is important to determine the diseased region in order to avoid side effects on the surrounding tissues. For these reasons, suitable planning for therapeutic treatments of some diseases has been investigated.

In medical engineering, it is crucial to provide a biomedical system that is less damaging to the patient, faster in giving results and easier to use. As a result of these encouraging studies, scientists and engineers pursue the possibility of benefit from electromagnetism technology in innovative diagnostic and therapeutic strategies providing these conditions. They are also deeply interested in incorporating this technology into current systems. As can be seen from the studies so far, highly successful systems can be developed by using electromagnetic fields at microwave frequencies.

1.1 Purpose of Thesis

Even though diagnosis with electromagnetic technology would be applied to many diseases, it was seen that current studies mostly focused on cancer diagnosis. Using microwaves for diagnosis of diseases other than cancer is drawing attention of the researchers in these days. In this thesis, the possibility of diagnosis of urolithiasis (the formation of kidney stone) with the help of electromagnetic properties is evaluated. A machine learning aided classification tool for kidney stone, the third most common disorder of urinary tract, is considered. For this purpose, firstly, the dielectric properties of each kidney stone were measured at microwave frequencies. Using generalized Newton-Raphson method, Cole-Cole parameters for kidney stones were calculated from these measurement results.

After measurement part, classification of the stones was carried out with machine learning algorithms which were Artificial Neural Network (ANN) and k-nearest neighborhood (KNN). Calculated Cole-Cole parameters were used as inputs of these algorithms. In this part, firstly, normalization was performed to prepare the input values for the network. Then, the stone samples were categorized as training and test samples with 10-fold cross validation. After the networks were trained with training samples, output was obtained for each test sample. These output values gave the stone type of the samples. In this thesis, the success of the algorithms for our kidney stone samples shows that dielectric property can be used for determine the stone types.

In conclusion, classification of kidney stones with electromagnetic properties is possible and machine learning algorithms can be used successfully in this aspect. The study can be advanced to make it possible to tell the type of kidney stone when it is in body. Thus, new treatment modality for urolithiasis can be developed and precautions for avoiding repetition can be decided without extracting it.

1.2 Literature Review

Although the dielectric properties of biomedical tissues and biomaterials have been widely reported in the past decades [4], there are only a few studies on dielectric properties of kidney stones. These studies have been performed for various aims and with various dielectric measurement methods. The method used in [5] is parallel plate and in this technique, it is generally required kidney stones to be smashed into fine powder and then, to be made into pellets. Dielectric constant, dielectric loss, conductivity and resistivity values of growth struvite stones were measured at 30^{o}C - 80^{o}C temperature range and 1 kHz - 1 MHz frequency range by using impedance analyzer. It is aimed to develop new treatment modality determining the temperature and frequency required for stone fragmentation.

Similar technique was utilized in another study, [6], to analyze electret behavior and conductivity of natural kidney stones which were thought as imperative to stop the stone growth. They were investigated only depending on temperature. Other similar studies, [7] and [8], were carried out at close temperature and frequency range in hopes of finding new treatments. In these studies, the stone samples were coated silver and then, dielectric property parameters were measured with an impedance analyzer. As distinct from the others, the study, [8], was also aimed to compare the dielectric properties of powdered and solid kidney stones and their differences were reported.

In the study [9], dielectric properties of kidney stones at 1 Hz – 1 MHz frequency range were also measured on the phantoms prepared to understand their growth mechanism.

Another identical study [10] is performed with same measurement method in close frequency range in order to analyze the stiffness of urinary stones and to understand their fragmentation mechanism during lithotripsy. Since it is known from previous studies that calcium oxalate is the hardest stone having low fragility, its fragmentation process was also investigated separately in [11].

While all of these studies were completed at relatively small frequencies and only with parallel plate technique, there is another study, [12], performed with cavity perturbation technique. It was also different than previous works in terms of measurement frequency range which was 2 GHz – 3 GHz. The study aimed to show the dielectric property differences between stone types thinking that it could help the determination of the type. In terms of both measurement frequency and purpose of study, this study is the most similar to ours among the studies on dielectric properties of kidney stones.

In other respects, if the studies on analysis of kidney stones with artificial intelligence systems are considered, it will be seen that they only took advantage of their images. In [13], a special device was developed to lighten and take photos of stones. Then, these photos were classified a machine learning algorithm, random forest classifier, and the type of stone was determined. Another study aimed to diagnose kidney stone disease with the help of ultrasound imaging [14]. In this study, it was provided an artificial neural network to diagnose the disease by considering the differences between the images of healthy kidney and kidney with stone.

As can be seen, studies in the literature usually purposed to determine the dielectric properties of kidney stones and to use this information in determination of the stone type. Moreover, only parallel plate and cavity perturbation techniques have been employed to measure dielectric properties. On the other hand, works on classification of kidney stones where the intelligent systems are used have only made use of the images of the stones. When considering all of these properties that previous studies had, it can easily be said that this is an innovative study that will contribute to the literature.

2. KIDNEY STONE DISEASE

Urinary system is a body system which is responsible for removing urine, consisting of wastes and extra fluid, from the body. The system mainly provides keeping the pH level and body liquids in normal range. It also has an important role on pulling out pharmaceutical products that can be toxic, and regulating blood pressure and concentrations of electrolyte and water. In order to fulfill these functions, all parts of urinary tract need to work in correct order. Urinary tract is composed of kidneys, ureters, urinary bladder and urethra as illustrated in Figure 2.1 [15]. In humans, there are two kidneys that filter the substances in the blood. Urethra, a pair of tube-like structures, transports the urine from kidneys to urinary bladder. Urinary bladder is the part collecting urine and serving as a reservoir. Urine is finally released from the body by the mean of urethra.

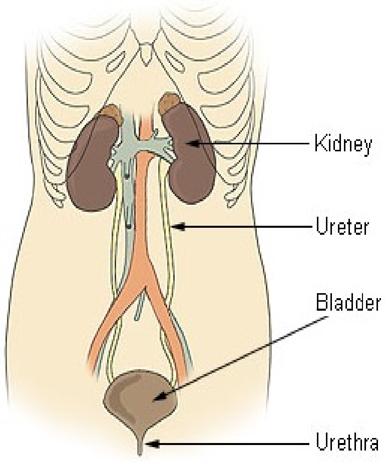

Figure 2.1 : Component of Urinary System in humans.

As it seen, the functions of urinary system are vital for human body and when there is a problem about them, it makes the patient's life difficult. Many people suffer from urinary tract diseases during his life. These diseases like urinary tract infections, kidney stones (urolithiasis), and prostate problems, reduce the quality of life. Some of these urologic conditions last only a short time, while the others are long-lasting [16]. The correct diagnosis and treatment of these diseases affect this recovery period. Moreover, recurrence can also be prevented with correct diagnosis. For this reason, developing new diagnostic methods and improving the current ones are the aims of many researchers. This study was started to develop a machine learning aided diagnostic tool for kidney stone disease.

Urolithiasis, the formation of kidney stones, have been seen in around 10% of the world population [17]. In Turkey, the prevalence of the disease is 11.2% in 2008 [18]. The recurrence rate can reach 40% in 5 years in some European countries [19]. Moreover, people whose first order relatives have had kidney stones are more likely to suffer from this disease. The nature of the geographical region which they live in also affects the incidence of the disease. All these factors taken into account, it can be said that the development of new methods for diagnosis, treatment and prevention of the disease is very important for world population.

Kidney stones are generally manufactured in kidneys, and can pass through all urinary tract. Small calcifications (Randall's Plaques) in the papilla of the kidney form the stones as seen in Figure 2.2 [20]. These formations are too small to be treated. When these calcifications grow and form the larger stones, they can be treated.

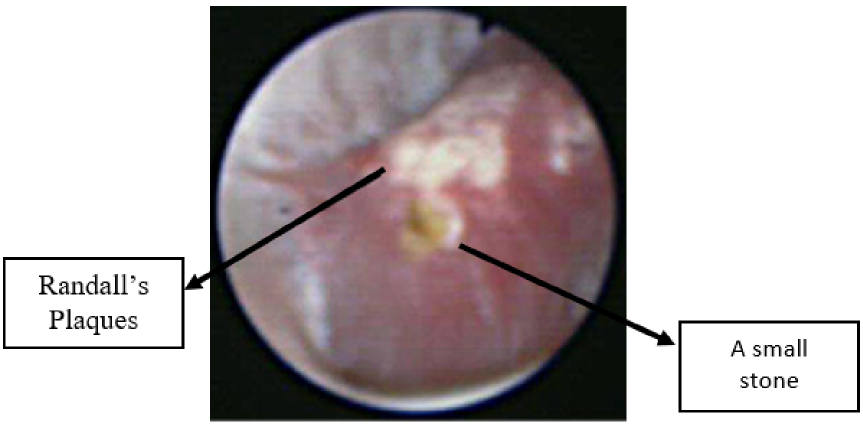

Figure 2.2 : Randall's Plaques and a stone arising from a Randall's Plaque in this view from a ureteroscope.

Urinary calcifications can be of different sizes, from a grain of sand to a few golf balls. Whether it is smaller or larger, same symptoms have been shown, but their severity may be different. The larger the stone, the more notable are the symptoms. More marked symptom is severe pain on either side of the lower back. When the stone causes irritation or blockage, extreme pain is felt. Additionally, continuous stomach ache, nausea or vomiting are seen in the presence of a kidney stone. Fever and chills in the body also appear. The form of the urine also changes; it smells bad and looks cloudy. Blood in the urine can also present. When patients have one of these problems, they consult to a physician and the disease is tried to diagnose.

2.1 Diagnosis of Kidney Stones

When a physician sees the patient with these complaints, he/she wants to know the medical history. After examining physically, exact shape and size of the stone is needed and obtained with imaging modalities. These modalities contain the use of X-rays such as Non-contrast Computed Tomography (CT) scan, an X-Ray of the Kidneys, Ureters and Bladder (KUB) and Intravenous Pyelogram (IVP); and the use of sound waves such as ultrasonography (US). Magnetic resonance imaging (MRI) is also utilized in this aspect [21].

CT is a cross-sectional imaging technique in which a series of X-ray projections of bones and soft tissues inside the body are obtained at different angles and processed. Thus, the images of the body part can be viewed in all anatomical planes. In CT scan, contrast agent, which absorbs more X-rays and provides better imaging, can be used for scanning of some parts of the body. For a patient with clinical suspicion of urinary stones, non-contrast CT is firstly used since it is the most accurate and rapid method for evaluating urinary calcifications. These characteristics of CT provide time savings and reduce the cost of treatment.

Intravenous pyelogram (IVP) uses an intravenous contrast agent that moving into the urinary tract and absorbs more X-rays. Difference between the absorption of X-rays by the stone and its surroundings that contains contrast agent is used in the formation of image and provides visualization of the stones. A disadvantage of this procedure is that preparing contrast agent takes time and delays the care. Furthermore, there are potential adverse effects of dye such as allergy. Since the non-contrast CT is adequate for stone imaging and has less disadvantages, this is a rarely used technique.

X-Ray for the Kidneys, Ureters and Bladder (KUB) is a planar radiography of abdominal area includes kidneys, ureters and bladder. In this method, radiation dose is much lower than CT. Rather than utilizing in first examination, it is preferred in the follow-up process of stone that do not need a surgical intervention. Since the modality is used for only radiopaque stones (detected by X-ray), some stones cannot be imaged with KUB. Moreover, airgap in the urinary tract also prevents the visualization.

Ultrasonography is imaging modality using the sound pressure waves produced by a probe. The probe is also collects the reflected waves and by processing these reflected signals, ultrasonographic image is obtained. Since non-ionizing radiation is used in this modality, it is preferred for children and pregnant women. US imaging also gives information about urine flow and the presence of obstruction caused by kidney stones. The sensitivity and specificity of the system for kidney stone is not higher than CT imaging. US cannot detect stones that is far away from the kidney or urinary bladder.

Magnetic resonance is simply a big magnet used for measurement of the water density in tissues and producing an image. MRI does not use ionizing radiation and it is especially used for pregnant patients when US imaging does not detect the stone. It also provides information about general health condition of urinary system if the pain is not caused by kidney stone. However, because of poor sensitivity for kidney stones and the higher cost of scanning, it is not usually chosen.

In summary, after the evaluation of doctor based on the medical history and physical examination, proper imaging technique is chosen. By taking all findings into consideration, treatment method is also determined and applied. The treatment process needed to apply depends on not only size and location of the stone, it also depends on the type of the stone. For this reason, types of kidney stones are investigated in the following section before possible treatment methods for urinary tract disease are explained.

2.2 Types of Kidney Stones

The human body can form a variety of different stone types. Calcium oxalate, struvite, cystine and uric acid are the most common stone types [21]. Other stone types are rare and do not covered in this thesis.

Most common type of urinary stones is calcium containing ones. These stones mainly consist of calcium oxalate. In some of patients, the calcium oxalate stone disease is secondary seen with hyperparathyroidism, hereditary hyperoxaluria, renal tubular acidosis, sarcoidosis, Cushing syndrome, steroid treatment, Vitamin D intoxication, immobilization and medullary sponge kidney disease. On the other hand, the stone disease is primary in majority of the patients.

Struvite stones also take place in the literature as infection or Magnesium Ammonium Phosphate stones. The incidence of struvite stones is 10–15% of all kidney stones. Since women are more prone to have urinary tract infections, the probability of these stones to occur in women is twice that in men. The infection associated with struvite stones is caused by urease-splitting bacteria.

Cystine in the urine is a genetic error of metabolism which causes the reabsorption of four amino acids, cystine, ornithine, lysine and arginine from renal tubular. Among these amino acids, only cystine contributes the stone formation due to its poor solubility. 1-2% of all renal stones belongs to this class. However, since it is an inborn disorder, 6-8% of stone cases seen in children.

Uric acid stones represent 5-10% of urinary calculi and they are more common in men than women. 25% of patients with uric acid calculi also have gout which affects uric acid metabolism in the body. The formation of the stones is also related with obesity and diabetes. Moreover, the most common cause of the formation is low urine pH.

2.3 Treatment of Kidney Stones

When the presence of the urinary stones is reported, proper treatment should be applied to the patient. The treatment is selected according to type, size and location of the stone, in addition to medical history of the patient. The stone can be tackled with using medicine, Extracorporeal Shockwave Therapy (ESWL), Percutaneous Nephrolithotomy (PCNL), ureteroscopy and open surgery [21].

It is known that patient's history and anatomical condition affect determination of treatment method. For example, an older man with enlarged prostates can pass his stone with the help of medication. In such cases, medication therapy is preferred instead of invasive or minimally invasive treatments. A type of medicine that dilate the ureter and ease the passage of the stone has recently been preferred since it eliminates the need for surgical treatments.

Extracorporeal Shockwave Therapy (ESWL) is a non-invasive technique applied for kidney stones. Shock waves, which are ultrasound waves produced outside the body, are transmitted to the kidney stones and these stones are broken into small pieces by the waves focusing on them. Small pieces of stones are removed from the body with urine in several days. In order to target the stones, ultrasound or fluoroscopy imaging is utilized. It is a less time-consuming and do not cause any incisions. A disadvantage of this technique is that it cannot be used for hard stones such as cystine and calcium oxalate. This treatment method has still been investigated and some reports claim that ESWL increases the risks for diabetes and hypertension.

Percutaneous Nephrolithotomy (PCNL) is a treatment method in which a tube is placed on back of the patient and the stones are extracted with a telescope through this tube. Before the stone is removed, it is broken into small fragments since extraction of these fragments are easier. Thus, very large stones and multiple small stones can be removed with PCNL easily. After this operation, it can be needed that the tube remains on the back of the patient for several day and it can be uncomfortable.

Ureteroscopy is a treatment method in which an ureteroscope is advanced through the urinary tract and reaches the kidneys. Through the scope, a powerful laser is applied and the stone is shattered into smaller pieces that are extracted with micro-baskets deployed through the scope. Since the procedure is minimally invasive, there is no incisions and need for hospitalization. However, it is not useful for large stones.

Open surgery for kidney stone was commonly preferred procedure in the past. Since other techniques have been developed, it started to be rarely chosen. If the stone is larger than 2 cm and other techniques did not work, the urologist need to perform an open surgery especially for the cases in which the stone blocks all the kidney. The stone is removed from the incision in the renal pelvis. In some cases, the kidney is divided longitudinally into two in order to extract the stone. In this procedure, the kidney is completely purified from the stones. However, since it is an invasive procedure, there are risks for infection, blood-loss and losing kidney functions. Moreover, it is uncomfortable for patient because a scar is left after operation and hospital stay must be required.

The kidney stone disease can treated with one of these methods according to size, shape, location and type of it. It is important to choose the treatment method that is the least risky and affects the daily life of the patient least. Since the recurrence risk is 80%

over the patient's lifetime, precautions should be taken to avoid after the disease has been treated. Prevention methods which are also differentiate with type of the stone are explained in the following section.

2.4 Prevention of Kidney Stones

It is crucial to determine the reasons for stone formation in order to take necessary precautions to avoid kidney stone formation. Especially for the people who have a case history about kidney stones, these measures can be life-saving. 24-hour urine test, blood test and stone analysis are the diagnostic methods applied in this respect [21].

A 24-hour urine test is performed for identifying the possible causes of the stone formation. The presence of blood, bacteria and leukocytes and in the urine is checked. Since a single specimen is inadequate for checking these parameters, urine collecting in 24-hour. The result of the analysis give necessary information to the urologist whether the cause of the stone is metabolic factors, diet or any other conditions. For instance, this test gives an idea about how the body use the fluid and whether the body is dehydrated. In this regard, this is important since dehydration increases the risk for stone formation.

A blood test, in which the levels of calcium, sodium, potassium, creatinine, uric acid and nitrogen are investigated, is also applied to decide appropriate precautions to keep away from reoccurrence of kidney stone. These tests inform physicians about metabolic condition of the kidneys and help them to correct the abnormalities. When this information is combined with the stone type, necessary protections can be advised to the patients.

Classifying the stone in order to choose the correct treatment and prevention method is most significant part of kidney stone story. The stones leave from the body by itself or by a physician. If the stone is small and do not show any symptoms, it can pass with urine after a conservative care. If shock wave lithotripsy is need to remove the stone, the stone fragments also pass with the urine. In such cases, the urine should be collected in a cup in order to carry out the stone analysis. The extracted stone is sent to pathology for evaluation and determination of the type of it. Knowing the type of the stone, future stone formation can be prevented with correct procedures.

Applying all these tests, metabolic factors that cause the stone formation can understand with stone analysis. If all the findings tell us the stone is calcium oxalate, a specific dietary is advised to the patient. Moreover, medical treatment is applied for metabolic abnormality if there is. Provided that the stone is struvite, it means there is infection in the urinary tract. In this case, antibiotic suppression is applied after stone extraction. Antimicrobial therapy and urinary acidification help to inhibit stone recurrence. For the patients who have struvite stone stories, increasing fluid intake and close follow-up have been suggested. The precautions to prevent uric acid stone formation are increasing the urinary pH and the urine volume. Medical therapy and dietary can also be needed. Since the cystine stones are caused by the presence of cystine in the urine, medical therapy is based on decreasing its concentration, increasing its solubility and decreasing its excretion.

In conclusion, urinary stone analysis is required together with blood and urine tests in order to take necessary measures. For this reason, scientists have been trying to improve current urinary stone analysis methods and to develop new ones. Current stone analysis tools and their properties are handled in the Section 2.5.

2.5 Current Methods for Determination of Stone Types

Determination of kidney stone types is needed to choose the appropriate treatment and prevention ways. For this purpose, several methods that utilize different characteristics of the stones have been developed and used. Chemical Analysis, Thermogravimetry, Optic Polarizing Microscopy, Scanning Electron Microscopy (SEM), Infrared Radiation (IR) Spectroscopy and X-Ray Powder Diffraction (XRD) are the currently available methods for stone analysis [22].

Chemical Analysis is one of widely used techniques for stone analysis. Commercial kits for performing chemical analysis of kidney stones have been developed and used in the laboratories. Individual ions and radicals in the stone can be identified with these kits. Uric acid, ammonium urate, cystine, calcium carbonate, calcium oxalate and calcium phosphate are the ions which are checked. The type of stone is determined from this ionic content. While this method is cost-effective, it takes a long time and it cannot distinguish compounds.

In thermogravimetry analysis, temperature of the stone is increased and weight change is recorded. Each stone has different transformation temperatures since its content is also different. Thus, the amount of change in weight will also be differ. In thermogravimetry analysis, this difference gives us the content, hence the type of stone. Unfortunately, this method is not very sensitive, and the stone is not recovered since it undergoes transformation.

Analysis with optic polarizing microscopy based on the interaction of polarized light with the stones. The stones are broken down and refractive index liquid is dropped onto fragments. Then, it is investigated under the polarizing microscope and some features like color, refraction of light and double refraction of light are determined. These parameters identify the type of stone, but discrimination of the components of the stones might be difficult.

In analysis with Scanning Electron Microscopy (SEM), the beam of high energy electrons is sent to the surface of the stone and an image is obtained from different signals derived from interaction between sample and electrons. Once images of each stone texture are distinct, the stone type can be detected. Disadvantage of this technique is the cost of it.

Infrared Radiation (IR) is used in order to vibrate the atoms of stone sample. Since the energy absorbed by each atom varies, the absorbance energy spectrum of each stone is also different, hence the stone is identified. The problem in this method is that the absorbance range of some components may overlap and so, the stone type cannot be distinguished. Similar analysis is carried out with X-Ray Powder Diffraction (XRD). In this method, monochromatic X-rays transmitted to the stone sample and the unique diffraction patterns are used to categorize the stones. This technique is the most common, but expensive one.

All methods explained in this section are currently performed for classify the stones. However, some problems about cost, usability, efficiency and sensitivity have been experienced. In addition to them, stones is damaged in most of techniques and this does not allow future analysis when necessary. Due to these reasons, new modalities have been searched in order to categorize the urinary calcifications.

3. ELECTROMAGNETIC PROPERTIES OF BIOLOGICAL TISSUES

The interaction of electromagnetic fields with biological materials at microwave or radio frequencies have been investigated with an increasing interest. It is crucial to know electromagnetic features of materials in order to understand how electromagnetic energy is coupled into biological systems and thus, diagnosis and treatment modalities benefiting from the interactions between biological materials and electromagnetic field can be developed. These interactions are currently used for some purpose such as tissue imaging [23] and tissue classification [2].

Electromagnetic properties, which affect the propagation of electromagnetic waves through tissues or biological materials, can be classified as magnetic and electrical properties. While permeability is a magnetic property of the material, permittivity and conductivity are the electrical ones. Permeability is the ability of the material to form magnetization within itself when magnetic field is applied whereas permittivity is the measure of resistance in responce to applied electric field. Another electrical property is conductivity which characterize how the electric current moves into a material. In this work, permittivity (dielectric property) of kidney stones is used for classification and therefore, only this property is discussed in detail.

3.1 Dielectric Property of Biological Substances

The interaction between electromagnetic fields and materials are described by Maxwell's equations (Equations 3.1-3.4) [24]:

$$\nabla x E = -\frac{\partial B}{\partial t} \tag{3.1}$$

$$\nabla x H = j + \frac{\partial D}{\partial t} \tag{3.2}$$

$$\nabla . D = \rho_e \tag{3.3}$$

$$\nabla.B = 0 \tag{3.4}$$

where E is electric field strengths, H is magnetic field, D is dielectric displacement (electric flux density), B is magnetic induction, j is the current density and ρ_e is the density of charges. When a material undergoes a time dependent process, there is a difference between time dependencies of electric field and dielectric displacement because of the molecular content of the material. As a result of this manner, it can be said that electric field, E, and dielectric displacement, D, depend on time or frequency.

Considering small electric fields, some deductions are made from the equations 3.1-3.4 and dielectric displacement, D, can be expressed as

$$D = \varepsilon E \tag{3.5}$$

where ε is absolute permittivity of the material formulated as

$$\varepsilon = \varepsilon^* \varepsilon_0 \tag{3.6}$$

where ε^* is relative permittivity and ε_0 is permittivity of free space which equals to $8.85x10^{-12}$.

Relative permittivity of a material, ε^*, or dielectric constant are the permittivity of material relative to free space. It is the measure of the ability to carry the electric field and to polarize in response to an electric source. In other words, it means how easiliy the material becomes polarized by applied electric field. The relative permittivity of the material is a complex quantity and expressed as

$$\varepsilon^*(w) = \varepsilon^{'}(w) - j\varepsilon^{''}(w) \tag{3.7}$$

where the real part, $\varepsilon^{'}$, is the measure of how much energy is stored from electric field and the imaginary part, $\varepsilon^{''}$, is the loss factor which means how much energy is lost because of dissipative forces when an external electric field is applied. All the parameters are the function of angular frequency, w.

Another deduction that can be made from equations 3.1-3.4 is for current density, j,

$$j = \sigma E \tag{3.8}$$

where σ is electrical conductivity, and E is electric field.

Electrical conductivity, σ, is a measure of how the electric current moves into a material. It is the ability to transmit electricity. It also depends on the atomic and molecular structures of the material [24]. According to the equations 3.2 and 3.5, current density is equal to time derivative of dielectric displacement and the conductivity can also be expressed in terms of dielectric loss

$$\sigma = iw\varepsilon^{''} \tag{3.9}$$

where w is angular frequency.

3.2 Dielectric Relaxation Theory

The polarization of a material to which an electromagnetic field is applied occurs with limited rates. When the frequency of applied electric field increases, the molecules cannot no longer rotate fast enough and become relaxation. This process is related with reduction of permittivity and referred as relaxation process. The expression for the dielectric constant in relaxation process was derived by Debye as

$$\varepsilon^{*} = \varepsilon_{\infty} + \frac{\varepsilon_s - \varepsilon_{\infty}}{1 + iw\tau} \tag{3.10}$$

where ε_{∞} and ε_s are dielectric constants measured at higher and lower frequencies, respectively, w is angular frequency and τ is relaxation time. From this equation, real and imaginary parts of dielectric constant can be written as follows [25]:

$$\varepsilon^{'} = \varepsilon_{\infty} + \frac{\varepsilon_s - \varepsilon_{\infty}}{1 + w^2\tau^2} \tag{3.11}$$

$$\varepsilon^{''} = \frac{(\varepsilon_s - \varepsilon_{\infty})w\tau}{1 + w^2\tau^2} \tag{3.12}$$

If it is aimed to eliminate the term, wτ, from equations 3.11 and 3.12, a circle equation in $\varepsilon^{'}$-$\varepsilon^{''}$ plane is obtained as follows:

$$(\varepsilon' - \frac{\varepsilon_s + \varepsilon_\infty}{2})^2 + (\varepsilon'')^2 = (\frac{\varepsilon_s - \varepsilon_\infty}{2})^2 \quad (3.13)$$

Since ε'' cannot be negative, only the semicircle of equation 3.13 over which ε'' is positive is considered and plotted as shown in Figure 3.1.

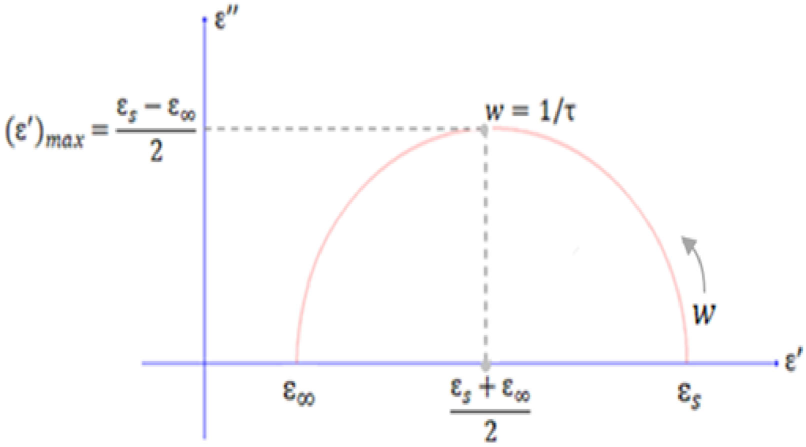

Figure 3.1 : Diagram of ε'-ε'' relation for Debye relaxation

In Debye equation, it is assumed that all dipoles have same relaxation time, τ, for simplicity. However, it is not sufficient to describe relaxation process of dielectric materials since there is a distribution of relaxation times. For this reason, Cole and Cole took the distribution of relaxation times into account and expressed the ε'-ε'' relation as follows:

$$\varepsilon^*(w) = \varepsilon_\infty + \frac{\varepsilon_s - \varepsilon_\infty}{(1 + iw\tau)^{(1-\alpha)}} \quad (3.14)$$

where α represents the distribution of relaxation time. The plot of this equation in ε'-ε'' plane is also semicircular, but the centre of the semicircle would be below ε''=0 axis at an angle, $\frac{\alpha\pi}{2}$.

In the literature, dielectric properties of biological tissues and related samples are widely described with a Cole-Cole model that also contains a conductivity term [4]:

$$\varepsilon^*(w) = \varepsilon_\infty + \frac{\varepsilon_s - \varepsilon_\infty}{(1 + iw\tau)^{(1-\alpha)}} + \frac{\sigma_i}{iw\varepsilon_0} \quad (3.15)$$

where σ_i is ionic conductivity of the sample.

3.3 Dielectric Property Measurement Techniques

As dielectric property can be a distinguishing property, its determination for biological materials have great importance for diagnosis of diseases as well as providing knowledge about the interaction between material and electromagnetic waves that can be used for therapeutic purposes. In order to measure dielectric parameters at microwave frequencies, many techniques have been developed based on the structure of measured material and the frequency range to be measured. These techniques are mainly resonant cavity perturbation, parallel plate, free space, transmission line and coaxial probe [26].

Resonant cavity perturbation technique utilizes from resonant cavities in which electromagnetic waves are oscillated and the waves would be stronger at resonance frequencies. of the cavity. When a material is placed into the cavity, the resonance frequency and quality factor, Q, is affected. From the change in these parameters, complex permittivity and permeability are determined at a single frequency. The system consists of a cavity and a network analyzer. The main disadvantage of the system is that the measurement is only carried out at a single frequency.

Secondly, the permittivity value can be determined by using parallel plate. Since the capacitance value is directly proportional with permittivity, a thin sheet of material placed between metal electrodes and the capacitance value is measured. Then, permittivity value of the material can be calculated. Measurement system is composed of a LCR meter, metal electrodes and an electrode fixture. This method is best for thin specimens and measurements at small frequencies.

The third is free space in which at least two antennas are used. One of the antennas sends the microwave or radio-frequency waves and the other receives the reflected waves. Antenna configuration can be straight or circular. In this method, S-parameters are measured and permittivity parameters are calculated from them. This conversion carried out with a software that can be set up into a network analyzer or an external computer.

The other method is transmission line in which the material is placed. The shape of line can be a section of rectangular waveguide or coaxial airline. The line is connected to the network analyzer and microwaves of radio-frequency waves are transmitted to the material. Then, S-parameters are measured and thus, the dielectric property values can be calculated. The measurement can be done at frequencies in a broad range.

The last one is coaxial probe that is an open ended section of transmission line. The measurement done by immersing the probe into liquid specimen or direct contacting with solid material. In this method, the wave is transmitted and reflected wave is measured via the probe. This system is covered in detail in the following section.

3.3.1 Dielectric Property Measurement System via Open-ended Coaxial Probe

Open-ended coaxial probe has been widely preferred to measure dielectric properties of biomaterials since it is a non-destructive method. The system is rough and measurements can be performed at any physical conditions like broad range of temperatures. Measurement with this technique requires the material to be in contact with probe and no-air gaps between them. For this reason, contacting face of the solid materials must be flat. Getting contact with the material, electromagnetic field at the probe is sent to the material and the reflected signal which is related to the permittivity of the material is measured. Measurements can be carried out at a wide range of frequency. The measurement system is composed of a network analyzer, a probe, a probe stands, a software and an external computer as seen in Figure 3.2.

A vector network analyzer is frequently used device in microwave measurements like dielectric measurements. It consists of a signal source, a receiver and a display. The source produce and send the signal at a single frequency and the receiver measures the signal reflected from the material. The magnitude and phase of scattering parameters (S-parameters) at that frequency are calculated. Then, the frequency is tuned to the next values and measurements are repeated for each value. The results are displayed as a function of frequency. The network analyzer launches the signal to the material by means of open-ended coaxial probe. This probe is a waveguide composed of two coaxial cylindrical conductors as shown in Figure 3.3.

The permittivity value of the material can be calculated with the help of this geometry and measured S-parameters by the software. The software calculates the permittivity and the permeability values and displays the results in a convenient way via the external computer. How the software carries out these calculations are explained with the following equations.

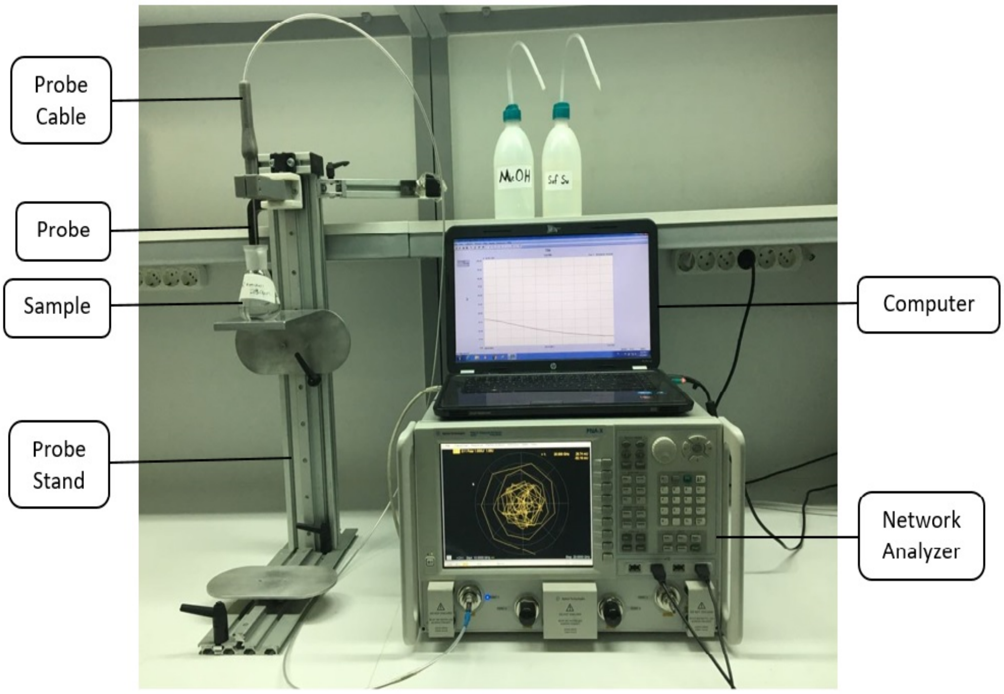

Figure 3.2 : Components of open-ended coaxial probe measurement set-up

Firstly, the normalized input admittance of the probe is needed to be written:

$$\frac{Y}{Y_0} = \frac{ik^2}{\pi k_c \ln(\frac{b}{a})} \int_a^b \int_a^b \int_0^\pi \frac{e^{-ikr}}{r} \cos\phi' d\phi' d\rho' d\rho \tag{3.16}$$

where

$$r = \sqrt{\rho^2 + \rho'^2 - 2\rho\rho' \cos(\phi)} \tag{3.17}$$

a and b are radius of inner and outer conductors, respectively, and k_c and k are wavenumbers inside the coaxial line and material, respectively. k_c and k are expressed as follows

$$k_c = w\sqrt{\varepsilon_c \varepsilon_0 \mu_0} \tag{3.18}$$

$$k = w\sqrt{\varepsilon^* \varepsilon_0 \mu_0} \tag{3.19}$$

where μ_0 is permeability of free space, ε_c is the permittivity of the dielectric material inside the probe and ε^* is the complex permittivity of unknown material.

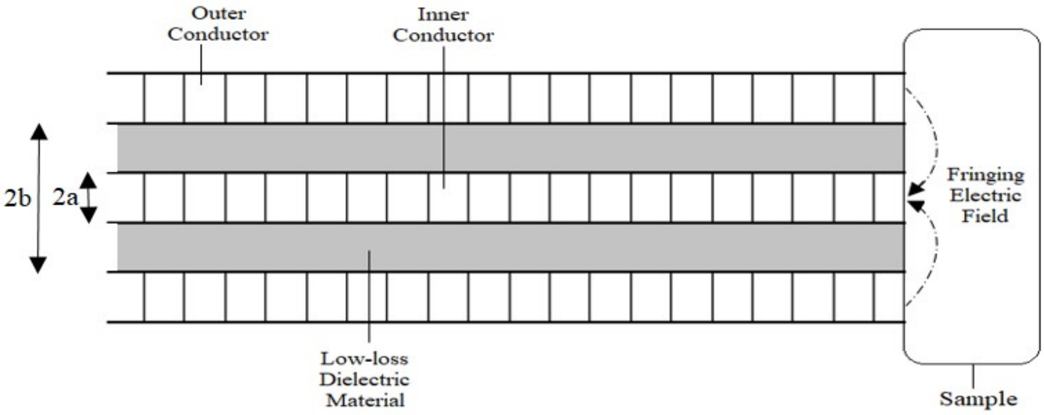

Figure 3.3 : Cross section of an open ended coaxial probe

When it is assumed that the coaxial opening of the probe is electrically very small, Equation 3.16 can be approximated by first few term of series expansion for exponential term and written as follows [27]:

$$\frac{Y}{Y_0} = \frac{ik^2}{\pi k_c \ln(\frac{b}{a})} \int_a^b \int_a^b \int_0^\pi [\frac{\cos\phi'}{r} - ik\cos\phi' - \frac{k^2 r}{2}\cos\phi' + i\frac{k^3 r^2}{6}\cos\phi'] d\phi' d\rho' d\rho \tag{3.20}$$

By using the relation between input admittance, Y, and characteristic admittance, Y_0, input admittance of the probe can be expressed as follows:

$$Y_0 = \frac{2\pi}{\sqrt{\frac{\mu_0}{\varepsilon_c \varepsilon_0}} \ln(\frac{b}{a})} \tag{3.21}$$

and

$$Y = i\frac{2w\varepsilon^*}{[\ln(\frac{b}{a})]^2}[I_1 - \frac{k^2 I_3}{2}] + \frac{k^3 \pi w \varepsilon^*}{12}[\frac{b^2 - a^2}{\ln(\frac{b}{a})}]^2 \tag{3.22}$$

where

$$I_1 = \int_a^b \int_a^b \int_0^\pi \frac{\cos\phi'}{r} d\phi' d\rho' d\rho \tag{3.23}$$

and

$$I_3 = \int_a^b \int_a^b \int_0^\pi \cos\phi' r d\phi' d\rho' d\rho \tag{3.24}$$

The second term of equation 3.22 goes zero on the integration over ϕ' and equation 3.22 becomes

$$Y = i\frac{2w\varepsilon^*}{[\ln(\frac{b}{a})]^2}[I_1 - \frac{k^2 I_3}{2}] \tag{3.25}$$

As seen in 3.23 and 3.24, I_1 and I_3 are independent from the material and only depend on the physical dimensions of the probe.

Secondly, it is known that the admittance, Y, can also be calculated with the following formula:

$$\frac{Y}{Y_0} = \frac{1+\Gamma}{1-\Gamma} \tag{3.26}$$

where Γ is the reflection coefficient of the probe calculated with the equation

$$\Gamma = \frac{\rho - S_{11}}{\rho S_{22} + S_{12}S_{21} - S_{11}S_{22}} \tag{3.27}$$

in which the S-parameters are measured with a network analyzer.

As a result, I_1 and I_3 are calculated numerically and the the admittance of the probe are also calculated from the measured S-parameters. By placing them into equation 3.25, the permittivity value, ε^*, can be calculated.

In conclusion, electrical and magnetic properties of biological substances are needed to be known in order to determine whether electromagnetic waves can be used into these substances for diagnostic or therapeutic purposes. These properties can be determined many different methods and measurement with open-ended coaxial probe is the newest and prevalent one. With the use of a network analyzer and a specific software, permittivity and permeability values of materials can be determined and used for further purposes.

4. MACHINE LEARNING ALGORITHMS FOR CLASSIFICATION

Many problems have been solved on a computer by using algorithms which contain the instructions that must be followed to transform the inputs to outputs. For some tasks like finding mean of inputs as output, necessary algorithm can be devised, but the exact relation between inputs and outputs is unknown for some applications, so the algorithm cannot be created easily. In such problems, patterns or regulations between them can be detected to make predictions about outputs. This process is provided by machine learning.

Machine learning is a part of artificial intelligence and it has the ability to learn [28]. It learns from example data or past experience and programs computers to optimize performance measure. Simply, machine learning teaches computers to make decisions. For this purpose, a mathematical model with some parameters are designed by using the theory of statistics and these parameters are optimized by using training data or experience. This model can be predictive or descriptive. It helps finding solutions for many problems such as data mining, natural language processing, image recognition, and expert systems. Machine learning models are classified in two categories according to the learning system. In supervised learning, training data containing the inputs and their corresponding outputs is used. The aim of computer is to detect the relation between input and output in training dataset, and determine the outputs of test inputs. Another category is unsupervised learning in which only inputs are present. In this learning model, the hidden pattern between inputs are revealed. It usually used for clustering or foreseeing how the process will continue.

Machine learning tasks can also be categorized depending on desired outputs. First of all, it is applicable for classification of inputs. An unknown input can be assigned to a class using the model designed by means of data with known results. Spam filtering is the best known example of classification. Support vector machines, decision trees, artificial neural networks and k-nearest neighborhood are the best known models for classification. Machine learning models are also suitable for clustering. The inputs can be clustered in accordance with their similarities by means of models such as k-means and self-organizing map. The other purpose of using machine learning is regression. It is used for prediction and outputs are continuous rather than discrete. An example for this is the estimating the number of vehicles that is sold in this year by looking the vehicle sales over the past few years and GDP for each year.

The features of the machine learning model to be used vary depending on the application. The input types, the presence of outputs, and the desired outputs determine which model will be more efficient to use. In this study, the purpose is classification of kidney stones. Inputs of the system are Cole-Cole parameters of the stones and the outputs are the types of them. Since the types of the stones are known, supervised learning model can easily be used. Considering these characteristics of the problem, it is understood that artificial neural network and k-nearest neighborhood (KNN) are suitable for this problem.

4.1 Artificial Neural Network

A neural network can be defined as a model of reasoning based on the human brain. The neural network consists of simple processors called as neurons which are similar to the biological neurons in the brain. The human brain consists of nearly 10 billion neurons and these neurons are connected to each other with synapses. A biological neuron consists of a cell body named as soma, a number of fibers named as dendrites, and a single long fiber named as axon. An artificial neuron also has similar structure shown in Figure 4.1 [29].

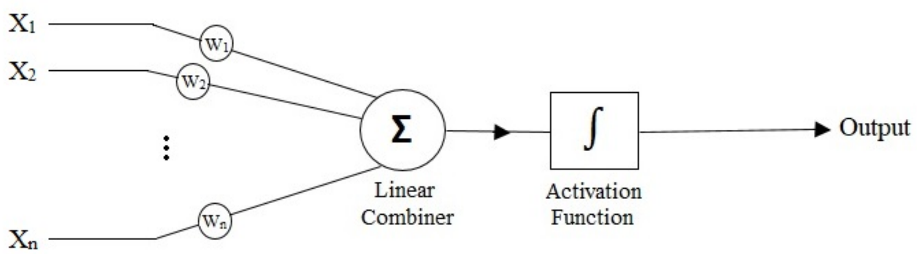

Figure 4.1 : Diagram of a single neuron

In Figure 4.1., inputs to the neuron represented by X_n and connection weights represented by W_n. The input signals of a neuron can be the features of the system or the signals came from another neuron. Each of these inputs is multiplied by corresponding weight and reaches the linear combiner which can be summation, minimum or maximum functions. In many cases, the linear combiner computes the weighted sum of inputs with following formula.

$$Sum = \sum_{i=1}^{n} X_i W_i \tag{4.1}$$

where i is the index starting from 1 to total number of inputs,n.

The output of linear combiner is passed from an activation function. This process corresponds to the work done by biological neurons. As the potential of input signals received by dendrites needs to be higher than the threshold potential to create an action, the result of the activation function determines the output of the process. The activation function can be various functions such as sign function, step function, sigmoid function or linear function based on the network design. Finally, the result of the activation function gives the output of the processing element. This output may be the output of the network or input of the other neurons. The output can split into a number of branches that transmits the same signal.

All artificial neural networks are constructed from these neurons, but they have different architectures based on the application. Simply, an artificial neural network is composed of one input layer, at least one hidden layer and one output layer as shown in Figure 4.2.

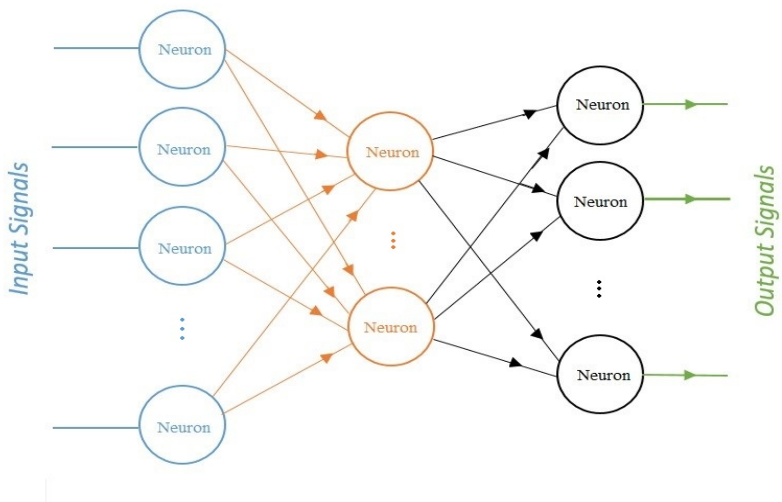

Figure 4.2 : Architecture of an artificial neural network

There is not any rule to determine the number of layers and the number of neurons in each layer of the neural network. In each layer, there may be different number of neurons which are connected by weights passing signals from one to another. Every neuron in input layer sends its output to each neuron in first hidden layer after performing its function. Similarly, the neurons in the hidden layer pass their outputs to all the neurons in next layer that can be another hidden layer or output layer. Finally, the neurons in output layer complete their process and get into competition with each other. This means a neuron inhibits the other neurons in the same layer to give output of the network. For example, in classification of iris flower, if the probability of being iris setosa is 0.87 and the probability of being iris virginica is 0.67, the network wants to prefer the highest probability and inhibit all the others. Apart from competition, there is another type of connection which is feedback. The output of one neuron routes back to the neurons in previous layer with feedback connection. This is an important part of training of the network which is covered in following section.

4.1.1 Training of Artificial Neural Network

The neural network can be trained with unsupervised or supervised procedures. In the unsupervised learning, the system groups the input data without knowing desired outputs and learns adaptively. On the contrary, both the inputs and the outputs are provided to the system in supervised learning. Since the supervised learning is used in this study, the procedure is discussed in detail.

After the network topology is determined, the input and output data is divided into two group as training and test. Then, the below steps are followed [28], [29]:

1. The connection weights are chosen randomly from a small range of $(\frac{-2.4}{F_i}, \frac{2.4}{F_i})$ where F_i is the total number of inputs of neuron i. If the weights are chosen large, the weighted sum also becomes large and the output of the transfer function becomes small. Since this output is used in weight training, the weight correction also becomes small. As a result, the training period lasts longer. To avoid this problem, the weights are initialized from small values on a neuron-by-neuron basis.

2. The inputs and outputs in the training dataset are given to the network and the neurons in input, hidden and output layers complete their processes.

- The outputs of the neurons in the hidden layer are calculated with the following formula:

$$Y_j = \begin{matrix} Activation \\ Function \end{matrix} \left(\sum_{i=1}^{n} X_i W_{ij} \right) \tag{4.2}$$

where n is the number of inputs of neuron j in hidden layer.

- The outputs of the neurons in the output layer are calculated with the following formula:

$$Y_k = \begin{matrix} Activation \\ Function \end{matrix} \left(\sum_{i=1}^{n} Y_j W_{jk} \right) \tag{4.3}$$

where m is the number of inputs of neuron k in output layer.

3. After having first outputs of the network, the weights are updated with with gradient descent backpropagation. In this step, the errors associated with the desired outputs, which are the outputs in the training dataset, are used.

   - The outputs of the neurons in the hidden layer are calculated with the following formula:

$$(W_{jk})_{new} = W_{jk} + \Delta W_{jk} \tag{4.4}$$

where weight correction, ΔW_{jk}, is calculated with

$$\Delta W_{jk} = \eta Y_j \delta_k \tag{4.5}$$

where η is learning rate and δ_k is error gradient with the formula

$$\delta_k = Y_k[1 - Y_k]e_k \tag{4.6}$$

where e_k is the error,

$$e_k = Y_d - Y_k \tag{4.7}$$

   - The weights at neurons in the hidden layer are updated with the following formulas:

$$(W_{ij})_{new} = W_{ij} + \Delta W_{ij} \tag{4.8}$$

where weight correction, ΔW_{ij}, is calculated with

$$\Delta W_{ij} = \eta X_i \delta_j \tag{4.9}$$

where η is learning rate from the range (0, 1) and δ_j is error gradient with the formula

$$\delta_j = Y_j[1 - Y_j] \left(\sum_{k=1}^{l} \delta_k W_{jk} \right) \tag{4.10}$$

where l is number of outputs of neuron k in output layer.

4. Since this is an iterative process, it is repeated from step 2 until the selected error criterion is satisfied.

After the training is completed with the data in training dataset, the inputs in test dataset is given to the network and their outputs can be obtained. Both inputs and outputs are needed to be numerical, suitable transformation can be necessary in some applications. Moreover, the number of neurons in the layers, the number of hidden layer and the learning rate is adjusted with trial and error. Despite this makes the design of network difficult, the network can learn to be adapted to the changes in the problem by this means. Considering all the advantages and disadvantages, artificial neural networks are widely used in many classification, clustering and recognition problems.

4.2 K-Nearest Neighbourhod

k-nearest neighborhood is a non-parametric method in which the same model is valid for all inputs. There is an important advantage of this method, having a small number of parameters needed to estimate to develop the model [28]. For example, only the k parameter, the number of neighbors taken into account, is determined for classification with KNN. Moreover, in this kind of model, it is assumed that similar outputs correspond similar inputs. For this reason, when the algorithm encounters an unknown data, it starts to investigate similar instances from testing set.

KNN algorithm uses the distance between the data to determine their similarities. As a distance measure, Euclidean relation, Manhattan relation or Minkowski relation can be used. In training phase, it places the data in training set into an appropriate coordinate system according to the data dimension. When the algorithm needs to find the class of an unknown input, it is also placed into the coordinate system and then, the classes of k neighbors, which are closest to it, are controlled. As a result, class of the unknown input is estimated from majority classes of neighbors.

Taking its similarity and usability into account, it can be said that KNN give highly competitive results. It can be easily applied for both classification and regression problems. Its applications range from political estimations to gene expression analysis. Working well in all kind of problems makes it highly preferred machine learning algorithm.

5. MATERIALS AND METHODS

Cole-Cole parameters of kidney stones are given an artificial neural network as inputs in order to classify them. To that end, electrical property measurements of the stones are performed with open-ended coaxial probe and Cole-Cole parameters are extracted from them by using generalized Newton-Raphson method. Then, these parameters are used in training and test phases of the network. Moreover, the stones are needed to be labeled since these labels are also essential in training. The properties of kidney stones and experimental setup used in this study, and applied measurement and classification procedures are detailed in the following sections.

5.1 Kidney Stone Samples

A total of 105 stones, the types of which are calcium oxalate, cystine and struvite, are measured in this study. There are 35 stones from each type ranging in radius from 0.25 to 1 cm. Some of them are showed in Figure 5.1. The removal of stones was done with one of various extraction methods which are ESWL, PCNL, ureteroscopy and open surgery.

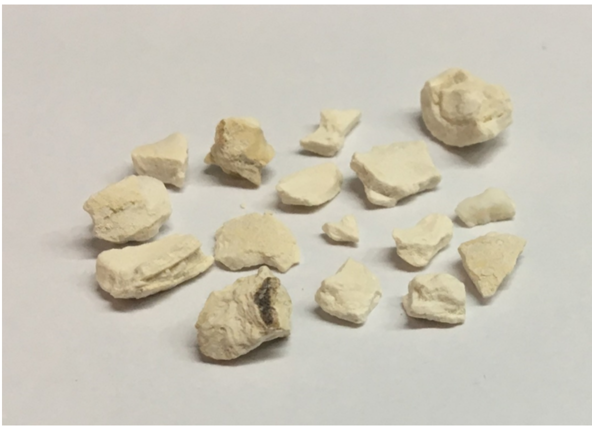

Figure 5.1 : Some of kidney stone samples.

Before the measurement utilizing from open-ended coaxial probe, the stones are needed to prepare. Since the probe is necessary to be a direct contact without leaving any air gap in order to measure the electrical properties of the stones more accurately, they were sanded to make their faces much smoother.

5.2 Experimental Setup

The dielectric property measurement system used in this experimental study is composed of Agilent N5242A PNA-X Microwave Network Analyzer, Agilent N1501A Dielectric Slim Form Probe, Agilent 85070E software and an external computer. Agilent N5242A PNA-X Microwave Network Analyzer is used to evaluate the magnitude and phase of scattering waves instead of directly measurement of electric field. The device has two ports with one source: the ports send the signal generated by the source and receive the reflected signals. The ports and corresponded scattering parameters are represented in Figure 5.2.

Figure 5.2 : Representation of the ports and scattering parameters in a 2-port VNA

As shown in Figure 5.1., 2-port VNA can measure four scattering parameters which are:

- S_{11} parameter corresponds to forward reflection. Signal is sent from port 1 and reflected back to port 1.
- S_{21} parameter corresponds to forward transmission. Signal is sent from port 1 and transmitted to port 2.
- S_{12} parameter corresponds to reverse transmission. Signal is sent from port 2 and transmitted to port 1.
- S_{22} parameter corresponds to reverse reflection. Signal is sent from port 2 and reflected back to port 2.

Although the device can produce and send signals at any frequency in the range of 10 MHz to 26.5 GHz, measurements are performed over the frequency range of 500 MHz – 6 GHz with 100 MHz intervals.

In order to carry the signals to the sample, Agilent N1501A Dielectric Slim Form Probe, which is an open-ended coaxial probe, is utilized. The probe has a slim design that enables to be used with smaller sample size. Its outer diameter is 2.2 mm and required to be used in samples that is at least two times bigger than its outer diameter [30]. Since it is used for the measurements in the frequency range 500 Mhz to 50 Ghz, it is quite suitable for use in this study.

The measured S parameters are needed to be converted into the permittivity of the sample. For this purpose, Agilent 85070E software is used on an external computer that takes scattering parameters from the vector analyzer. The algorithm that used in the software are summarized in Chapter 3. The software is also required a calibration process with air, a conductive textile and deionized water. Before the measurement, calibration must be performed carefully to obtain more accurate results.

5.3 Measurement Procedure

Before starting the measurement process, the slim form dielectric probe was sterilized with ethylene oxide and then calibration was carried out carefully according to the software instruction. In calibration, first the probe was left in the open air and dielectric property of the air was measured. Then, the measurement of short, a conductive material given in the software kit, was performed. Finally, the probe was inserted into a beaker of deionized water of which temperature was known. After making sure that there was no bubble in the tip of the probe, the dielectric property of the water was measured. This is a critical step because even a tiny bubble on the end of the probe can cause wrong calibration, and so wrong measurements.

After performing calibration, relative permittivity and conductivity measurements of water and pure methanol were performed at 23 °C and results were given in the Table 5.1. According to the table, it can be said that there was a good match between these measurement results and the literature data [2], [31], [32]. Thus, the probe performance was verified and the probe was ready for measurements of kidney stones.

Table 5.1 : Relative permittivity and conductivity measurements of water and pure methanol.

Frequency (GHz)	Deionized Water		Methanol	
	$\varepsilon^{'}$	σ (S m^{-1})	$\varepsilon^{'}$	σ (S m^{-1})
1	79.78	0.22	30.12	0.50
2	78.85	0.95	23.63	1.53
3	77.63	2.11	18.11	2.43
4	76.01	3.67	14.10	3.11
5	73.97	5.57	11.49	3.59
6	71.68	7.73	9.91	3.98

As previously explained, it is necessary to sand the surfaces of the kidney stones to flatten them, so that there is no air gap between the stone and the probe during the measurement. After being sure that the probe was in direct contact with the stone as shown in Figure 5.3, the measurement was done and the result was saved.

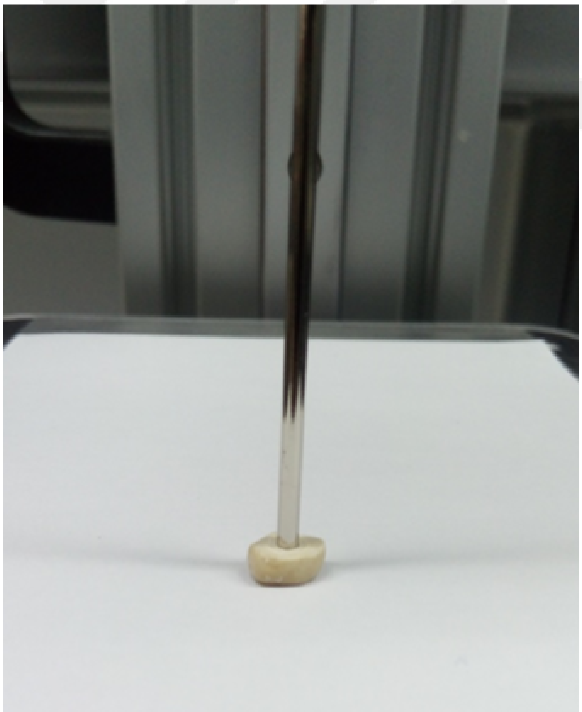

Figure 5.3 : Measurement of a cystine stone with open ended coaxial probe

Totally five measurements were performed for each type of the stone, and their medians were saved as $\varepsilon^{'}$ and $\varepsilon^{''}$ of the stone. Hence, the measurement part of the study was completed and data processing could be started.

5.4 Data Processing and Classification

After taking $\varepsilon^{'}$ and $\varepsilon^{''}$ values of all kidney stones between 500 MHz – 6 GHz frequency range, these values were needed to be fitted to Cole-Cole model. In order to do this, $\varepsilon^{'}$, $\varepsilon^{''}$ and their measured frequency value were placed into Cole-Cole equation.

$$g(w) = \varepsilon^{*}(w) = \varepsilon_{\infty} + \frac{\varepsilon_s - \varepsilon_{\infty}}{(1 + iw\tau)^{(1-\alpha)}} + \frac{\sigma}{iw\varepsilon_0} \tag{5.1}$$

Since measurements were taken at fifty-six frequency points, fifty-six equations were obtained. These equation set was solved for Cole-Cole parameters, which are ε_{∞}, ε_s, τ, α, and σ making use of the generalized Newton-Raphson (GNR) method. Because GNR is an iterative method making use of the partial derivatives of the equation to solve it, first values of ε_{∞}, ε_s, τ, α, and σ were assigned at the begining. Then, firstly the partial derivatives of the equation with respect to ε_{∞}, ε_s, τ, α, and σ and a scale matrix, c was calculated for each parameter as follows:

$$c = \begin{bmatrix} c_{\varepsilon_{\infty}}(w) \\ c_{\varepsilon_s}(w) \\ c_{\tau}(w) \\ c_{\alpha}(w) \\ c_{\sigma}(w) \end{bmatrix} = \begin{bmatrix} \frac{1}{max(\frac{\partial g(w)}{\partial \varepsilon_{\infty}})} \\ \frac{1}{max(\frac{\partial g(w)}{\partial \varepsilon_s})} \\ \frac{1}{max(\frac{\partial g(w)}{\partial \tau})} \\ \frac{1}{max(\frac{\partial g(w)}{\partial \alpha})} \\ \frac{1}{max(\frac{\partial g(w)}{\partial \sigma})} \end{bmatrix} \tag{5.2}$$

After then, a matrix N composed of scaled partial derivatives was written:

$$N = \begin{bmatrix} c_{\varepsilon_{\infty}}(\frac{\partial g(w_1)}{\partial \varepsilon_{\infty}}) & c_{\varepsilon_s}(\frac{\partial g(w_1)}{\partial \varepsilon_s}) & c_{\tau}(\frac{\partial g(w_1)}{\partial \tau}) & c_{\alpha}(\frac{\partial g(w_1)}{\partial \alpha}) & c_{\sigma}(\frac{\partial g(w_1)}{\partial \sigma}) \\ c_{\varepsilon_{\infty}}(\frac{\partial g(w_2)}{\partial \varepsilon_{\infty}}) & c_{\varepsilon_s}(\frac{\partial g(w_2)}{\partial \varepsilon_s}) & c_{\tau}(\frac{\partial g(w_2)}{\partial \tau}) & c_{\alpha}(\frac{\partial g(w_2)}{\partial \alpha}) & c_{\sigma}(\frac{\partial g(w_2)}{\partial \sigma}) \\ \vdots & \vdots & \vdots & \vdots & \vdots \\ c_{\varepsilon_{\infty}}(\frac{\partial g(w_{56})}{\partial \varepsilon_{\infty}}) & c_{\varepsilon_s}(\frac{\partial g(w_{56})}{\partial \varepsilon_s}) & c_{\tau}(\frac{\partial g(w_{56})}{\partial \tau}) & c_{\alpha}(\frac{\partial g(w_56)}{\partial \alpha}) & c_{\sigma}(\frac{\partial g(w_56)}{\partial \sigma}) \end{bmatrix} \tag{5.3}$$

In the following step, the difference between real value and calculated value of the complex permittivity was calculated:

$$R = \begin{bmatrix} \varepsilon^*(w_1) \\ \varepsilon^*(w_2) \\ \vdots \\ \varepsilon^*(w_{56}) \end{bmatrix} - \begin{bmatrix} g(w_1, {\varepsilon_s}^0, {\varepsilon_\infty}^0, \tau^0, \alpha^0, \sigma^0) \\ g(w_2, {\varepsilon_s}^0, {\varepsilon_\infty}^0, \tau^0, \alpha^0, \sigma^0) \\ \vdots \\ g(w_{56}, {\varepsilon_s}^0, {\varepsilon_\infty}^0, \tau^0, \alpha^0, \sigma^0) \end{bmatrix} \tag{5.4}$$

By using these matrices, error gradient vector was calculated with the formula,

$$\delta_g = [\delta_{g(\varepsilon_\infty)} \delta_{g(\varepsilon_s)} \delta_{g(\tau)} \delta_{g(\alpha)} \delta_{g(\sigma)}] = [\beta I + N^* N]^{-1} N^* R \tag{5.5}$$

where I is 5x5 identity matrix and $\beta = \frac{1}{100}$ (max | eig($N^{'}$N) |).

Then, new values of ε_∞, ε_s, τ, α, and σ could be calculated utilizing error gradient vector as follows:

$${\varepsilon_\infty}^1 = c_{\varepsilon_\infty} \delta_g(1) + {\varepsilon_\infty}^0 \tag{5.6}$$

$${\varepsilon_s}^1 = c_{\varepsilon_s} \delta_g(2) + {\varepsilon_s}^0 \tag{5.7}$$

$$\tau^1 = c_\tau \delta_g(3) + \tau^0 \tag{5.8}$$

$$\alpha^1 = c_\alpha \delta_g(4) + \alpha^0 \tag{5.9}$$

$$\sigma^1 = c_\sigma \delta_g(5) + \sigma^0 \tag{5.10}$$

These calculated values of the parameters were placed into the Cole-Cole equation and fitted dielectric properties, $\varepsilon^{'}$ and $\varepsilon^{''}$, were obtained. Finally, error of the process was calculated by utilizing Euclidean distance between fitted and measured data given in the formula:

$$error = \frac{1}{N} \sum_{i=1}^{N} \left[\left(\frac{\varepsilon^{'}_{w_i} - \hat{\varepsilon}^{'}_{w_i}}{median(\varepsilon^{'}_{w_i})} \right)^2 - \left(\frac{\varepsilon^{''}_{w_i} - \hat{\varepsilon}^{''}_{w_i}}{median(\varepsilon^{''}_{w_i})} \right)^2 \right] \tag{5.11}$$

where ε'_{w_i} and ε''_{w_i} are the measured dielectric properties, $\hat{\varepsilon}'_{w_i}$ and $\hat{\varepsilon}''_{w_i}$ are fitted dielectric properties and N is the number of points used within the frequency range of 0.5 GHz–6 GHz [2].

This process was pursued iteratively until finding the error below 0.02. After the stopping criteria was provided, Cole-Cole parameters for each stone were obtained and then, used for classification.

To classify kidney stones, machine learning algorithms, artificial neural network and k-nearest neighborhood, were developed and calculated Cole-Cole parameters were given as inputs to these algorithms. While ε_∞, ε_s, τ, α, and σ values for each stone formed five input vectors, the corresponding output vector was composed of their types. Since the outputs must be numerical, an output vector, in which 1, 2 and 3 were used for representing calcium oxalate, cystine and struvite, respectively, was created. Then, each vector was normalized in the range of (-1, 1) because normalization allows convergence to occur faster during training and the transfer function to work better.

After normalization, it was required to separate the dataset into two groups as training and test sets. This was performed utilizing k-fold cross validation, a well-known cross validation technique. In this step, k was selected as five and the data was split into five folds. The data in four folds was used for training the algorithms and then the algorithm was tested with the data in remaining folds. This process was repeated until each of the folds was used as testing fold.

Then, firstly, artificial neural network algorithm was developed in Matlab by determining the network structure. Since there are five inputs, input layer neuron number selected as five. As mentioned before, the number of hidden layers and the number of neurons in hidden layer were decided by trial and error. For this study, it was sufficient to contain one hidden layer with fifteen neurons. The activation function of this layer was preferred as tangent sigmoid function:

$$Y = \frac{1}{1+e^{-S}} \tag{5.12}$$

where S is input of the hidden layer neuron and Y is the output of the hidden layer neurons in the range of (-1, 1). Similar to the input layer, the number of neurons in output layer was also adjusted according to the number of outputs which was one for this problem. The activation function of output layer was selected as linear function.

After the architecture of network was specified as 5-15-1 network with tangent sigmoid transfer function in the hidden layer and linear transfer function in the output layer, the training of the network was completed with gradient descent algorithm as described in Section 4.1.1. Then, the data in testing folds was classified, and the performance of the algorithm was analyzed.

Secondly, KNN algorithm was also developed in Matlab environment in order to classify kidney stones. k parameter was selected as 5 by the way of train and error. The algorithm, then, was trained by using the data in training folds and outputs for inputs in testing fold were found. Consequently, outputs were investigated to learn whether the classification results were correct or not, and some performance measures such as accuracy, sensitivity and specificity were calculated to analyze the success of algorithm.

The performance of a machine learning algorithm is generally measured with the help of a 2-by-2 matrix called as confusion matrix. This matrix is composed of true positive (tp), false positive (fp), false negative (fn) and true negative (tn) counts in the classification. The meaning of these terms can be explained with an example from this study. A true positive means where a stone is classified as calcium oxalate when it should be classified as calcium oxalate. Unlikely, it is called false positive when a stone is not calcium oxalate and it is predicted as calcium oxalate. True negative test result is received when a stone classified as non-calcium oxalate while it is actually not calcium oxalate. False negative is another test result received when a calcium oxalate stone is classified as non-calcium oxalate.

In this study, following measures were calculated from confusion matrices:

- Accuracy is the ratio of correct predictions to all predictions.
  $$Accuracy = \frac{\sum tp + \sum tn}{\sum tp + \sum tn + \sum fp + \sum fn}$$
- Sensitivity is the ratio of positives which are correctly classified to actual positives.
  $$Sensitivity = \frac{\sum tp}{\sum tp + \sum fn}$$

- Specificity is the ratio of negatives which are correctly classified to actual negatives.
$$Specificity = \frac{\sum tn}{\sum tn + \sum fp}$$
- Precision is the ratio of positives which are correctly classified to all predicted positives. It depends on the reliability of positive results.
$$Precision = \frac{\sum tp}{\sum tp + \sum fp}$$
- Recall is the ratio of negatives which are correctly classified to all predicted negatives. It depends on the reliability of negative results.
$$Recall = \frac{\sum tn}{\sum tn + \sum fn}$$
- F1 Score is the weighted average of sensitivity and specificity. It is more useful to evaluate the reliability of classification.
$$F1\ Score = 2\frac{sensitivity * specificity}{sensitivity + specificity}$$

6. RESULTS

A dataset containing electromagnetic properties of 105 kidney stones extracted from 20 patients was used in order to evaluate the success rate of kidney stones classification with electromagnetic properties. According to kidney stone analysis results performed by several institutions like Directorate of Mineral Research and Exploration, these stones belonged to three distinct classes. These classes were calcium oxalate, cystine and struvite, and each class contained 35 stones.

6.1 Dielectric Measurement Results of Kidney Stones

Dielectric property measurement of each stone was carried out with open-ended coaxial probe. Median permittivity and conductivity values of the stones depending on frequency are shown through the graphs in Figure 6.1. Error bars on the graphs demonstrate standard deviations of permittivity and conductivity of the stones. As seen from the figure, standard deviations are high and some measurements of stone types overlap. For this reason, more than one measurements are carried out from each stone and their medians are used for classification to increase the accuracy.

To better illustrate the permittivity and conductivity differences between stone types, medians of their dielectric properties are summarized in the Table 6.1. In the measurement frequency range of 0.5-6 GHz, median permittivity of calcium oxalate is between 2.28-2.35 whereas median permittivity of cystine is in the range of 2.17-2.63 and the permittivity of struvite is in the range of 3.16-3.38. On the other hand, the conductivity of calcium oxalate is between 0.45x10^{-2} Sm^{-1} and 1.6x10^{-2} Sm^{-1}, while that of cystine is between 0.19x10^{-1} Sm^{-1} and 1.5x10^{-1} Sm^{-1} and that of struvite is between 2.0x10^{-2} Sm^{-1} and 3.5x10^{-2} Sm^{-1}. From the table, it can be concluded that the permittivity differences are more pronounced at lower frequencies while a clear distinction exists between the conductivity values at higher frequencies.

The conductivity and permittivity values presented in this study are close to the data in [12]. In this study, dielectric properties (ε', ε'') of calcium oxalate, cystine and struvite

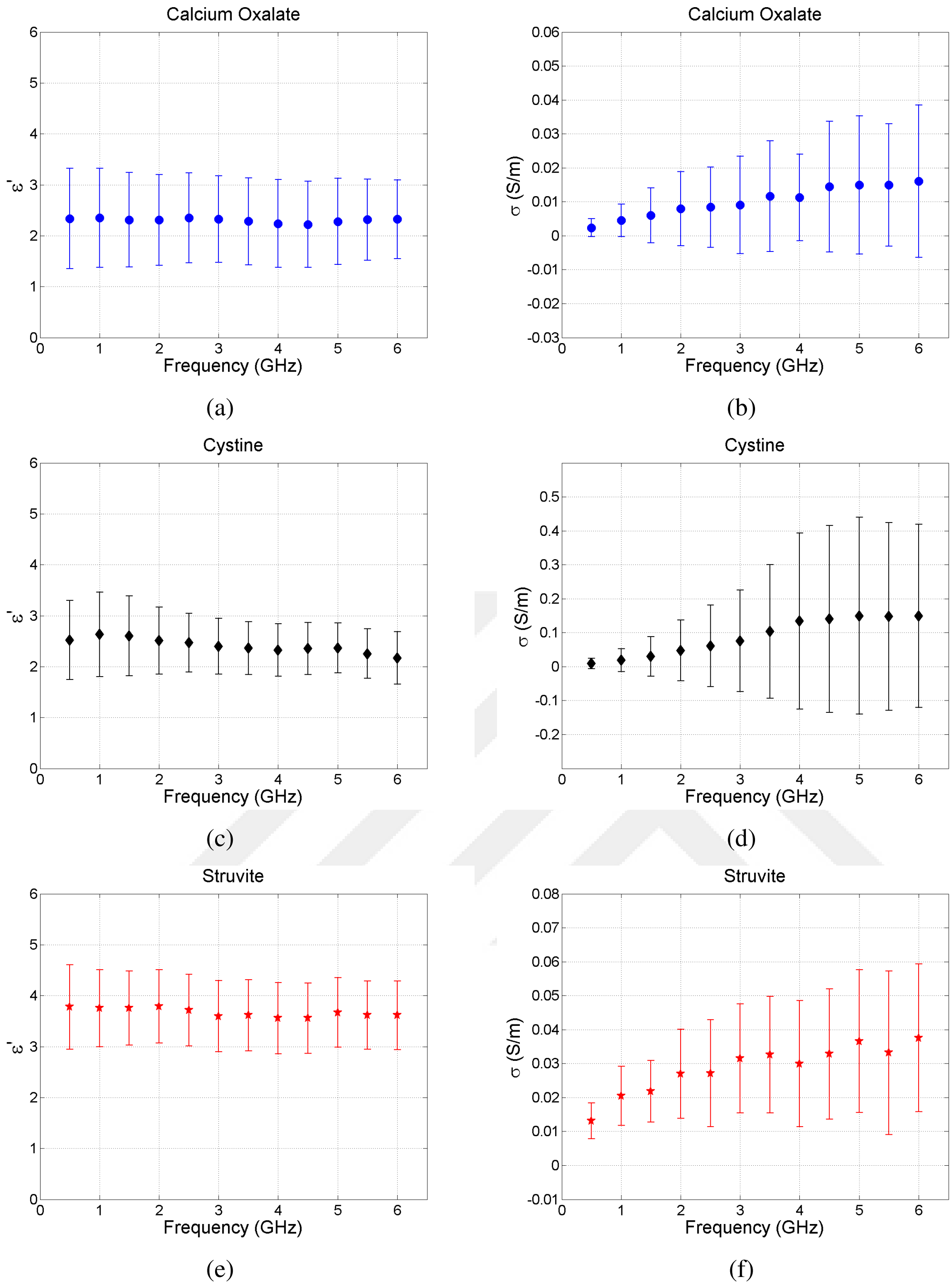

Figure 6.1 : Median in dielectric property measurements of kidney stone samples with variability bars: (a) Permittivity measurement of calcium oxalate, (b) Conductivity measurement of calcium oxalate, (c) Permittivity measurement of cystine, (d) Conductivity measurement of cystine, (e) Permittivity measurement of struvite, (f) Conductivity measurement of struvite.

at 2247 MHz are reported as (3.1, 0.37), (2.9, 1.09) and (4.2, 0.76), respectively. The same parameters for same stone types are measured as (2.33, 0.06), (2.51, 0.47) and (3.65, 0.25) at 2.3 GHz. The reason for small differences between reported data in these two studies can result from the frequency difference or measurement technique.

Table 6.1 : Medians dielectric property measurements of calcium oxalate, cystine and struvite stones.

Frequency (GHz)	Calcium Oxalate		Cystine		Struvite	
	$\varepsilon^{'}$	σ (S m^{-1})	$\varepsilon^{'}$	σ (S m^{-1})	$\varepsilon^{'}$	σ (S m^{-1})
1	2.3525	0.0045	2.6335	0.0190	3.3131	0.0199
2	2.3067	0.0079	2.5113	0.0481	3.3779	0.0269
3	2.3271	0.0091	2.3991	0.0760	3.2421	0.0265
4	2.2392	0.0113	2.3241	0.1342	3.1628	0.0275
5	2.2771	0.0150	2.3675	0.1498	3.3729	0.0303
6	2.3226	0.0161	2.1708	0.1491	3.2165	0.0349

6.2 Results of Cole-Cole Fitting to Dielectric Measurements

After the analysis of dielectric property measurements of kidney stones, Cole-Cole fitting is performed to the median of each stone type and Cole-Cole parameters are extracted with generalized Newton-Raphson numerical method described in Section 5.4. Median of measured relative dielectric constant and conductivity of each stone and their fitted lines are shown in Figure 6.2. It can be seen from the figure that there is a good matching between median and fitted data.

Fitted Cole-Cole parameters for each stone type are listed in Table 6.2 together with error rows. Similar to the relation between median dielectric constants of the stone types, struvite has the highest value for ε_{∞} and calcium oxalate has the lowest one. The same relation exists among σ values of the groups. However, when ε_s is the question, the highest value belongs to cystine while the lowest belongs to calcium oxalate. Moreover, it is easily seen from the table, τ and α values for calcium oxalate are the greatest and these values for struvite are the smallest. All these electromagnetic property discrepancies show that these properties can be used for classification of kidney stones.

6.3 Results of kidney stone classification

The dataset composed of Cole-Cole parameters of the stones as inputs and their types as outputs has been used for classification. Each attribute in the dataset has been normalized and used in ANN and KNN algorithms. As said before, 5-fold

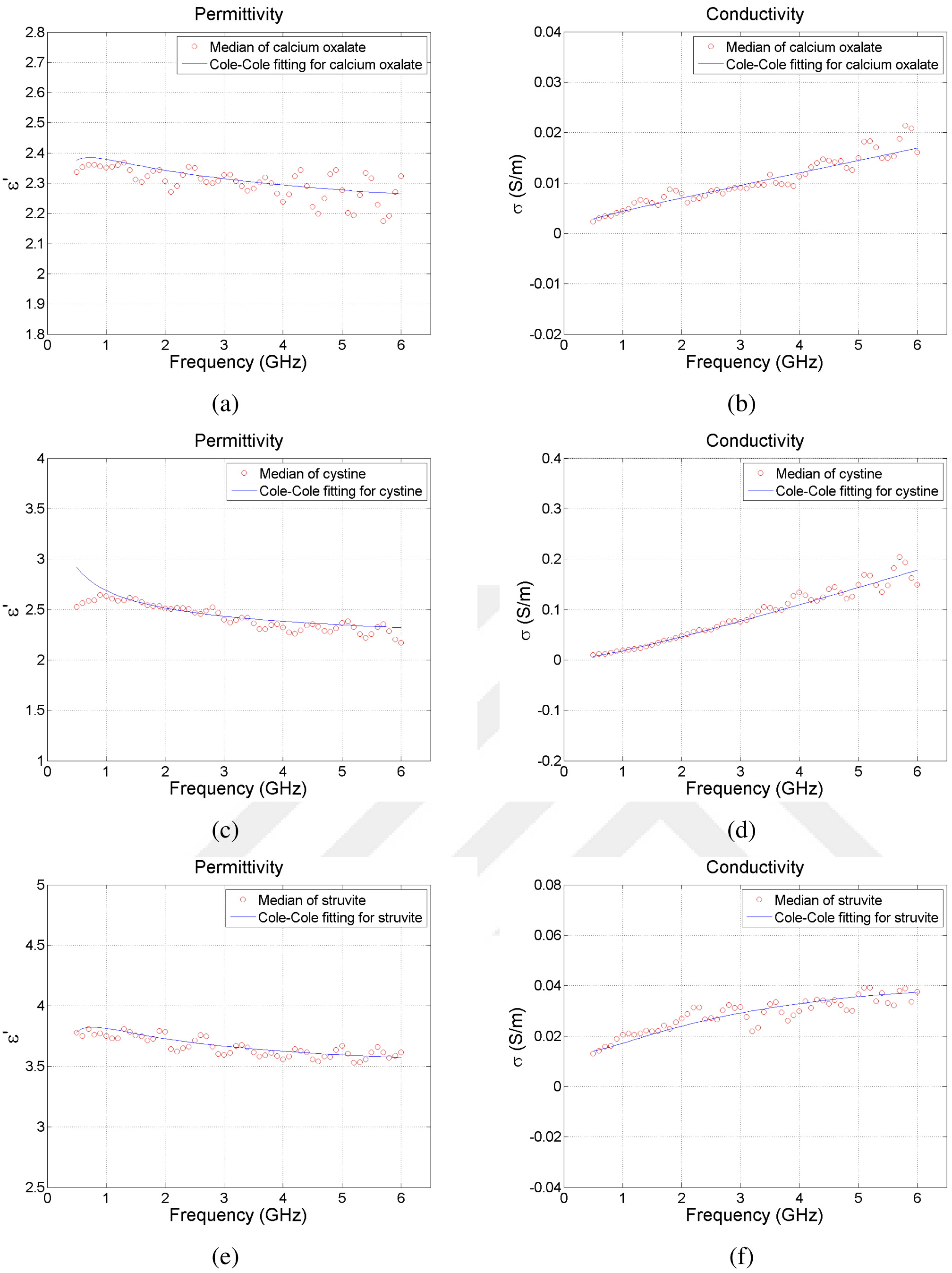

Figure 6.2 : Comparison of medians and Cole–Cole fittings: (a) Measured and fitted permittivity comparisons for calcium oxalate, (b) Measured and fitted conductivity comparisons for calcium oxalate, (c) Measured and fitted permittivity comparisons for cystine, (d) Measured and fitted conductivity comparisons for cystine, (e) Measured and fitted permittivity comparisons for struvite, (f) Measured and fitted conductivity comparisons for struvite.

cross validation has also been utilized in order to split the data into training and test groups. The classification results and analysis of these results are given in the following sections.

Table 6.2 : Cole–Cole parameters fitted to the median of each stone type.

Cole-Cole parameters	ε_∞	ε_s	τ	α	σ (S m^{-1})	error
CaOx	1.96	12.84	1.41e-06	0.73	8.11e-05	0.0151
Cystine	1.93	16.78	6.04e-07	0.62	0.0071	0.0111
Struvite	3.50	14.66	1.80e-07	0.39	0.0365	0.0099

6.3.1 ANN Results

ANN algorithm designed as stated in Section 5.4 is trained with the data in training folds and used for classification of the data in testing fold. Same training and test processes are repeated until whole folds are used for test, and classification results of all folds are collectively presented in following tables and figure. As seen from Table 6.3, all of the calcium oxalate stones are predicted as calcium oxalate, but one of cystine stones and one of struvite stones are wrongly classified as calcium oxalate.

Table 6.3 : Classification results for all stone types.

		Actual Class		
		Calcium Oxalate	Cystine	Struvite
Predicted Class	Calcium Oxalate	35	1	1
	Cystine	0	33	0
	Struvite	0	1	34

As stated before, the performance measures of a machine learning algorithm are calculated from 2-by-2 confusion matrix that contains tp, fp, fn and tn counts. These counts can be calculated for each stone by using the number of correct and wrong classifications. As a result, confusion matrices for stone types can be formed as follows to evaluate the performance of this algorithm.

The performance measures that can be calculated from these matrices are accuracy, sensitivity, specificity, precision, recall and F1 score. These measures are calculated and demonstrated with Table 6.7 and Figure 6.3. As seen from the table and the figure, all performance measures for ANN algorithm are above 97%. These results are quite promising and show that the algorithm can determine the type of stone from

Table 6.4 : Confusion matrix for calcium oxalate.

		Actual Class	
		Calcium Oxalate	non-Calcium Oxalate
Predicted Class	Calcium Oxalate	35	2
	non-Calcium Oxalate	0	68

Table 6.5 : Confusion matrix for cystine.

		Actual Class	
		Cystine	non-Cystine
Predicted Class	Cystine	33	0
	non-Cystine	2	70

Table 6.6 : Confusion matrix for struvite.

		Actual Class	
		Struvite	non-Struvite
Predicted Class	Struvite	34	1
	non-Struvite	1	69

its dielectric properties. By further increasing the performance, a new kidney stone analysis tool utilizing electromagnetic properties of the stone can be developed.

Table 6.7 : Performances of ANN for kidney stone classification.

Performance Measures	Calcium Oxalate	Cystine	Struvite	Whole
Accuracy	98.1%	98.1%	98.1%	98.1%
Sensitivity	100%	94.3%	97.1%	97.1%
Specificity	97.1%	100%	98.6%	98.6%
Precision	94.6%	100%	97.1%	97.2%
Recall	100%	97.2%	98.6%	98.6%
F1 Score	93.1%	97.1%	97.8%	96.0%

6.3.2 KNN Results

KNN algorithm is also designed as stated in Section 5.4 in order to use for kidney stone classification. The algorithm is firstly trained with the data in training folds and then,

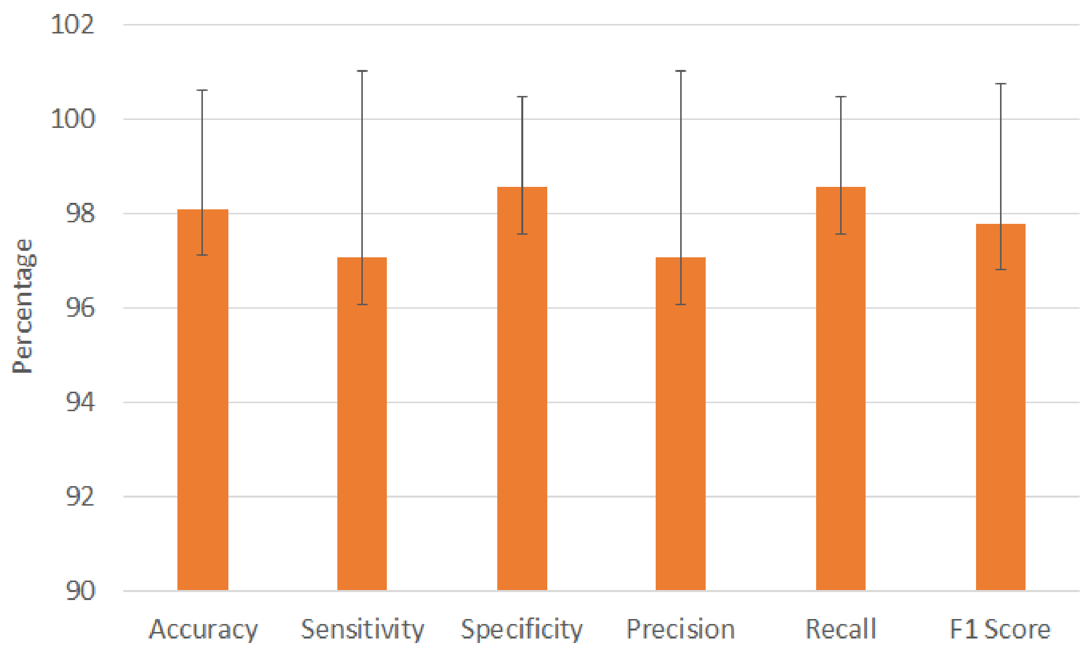

Figure 6.3 : Performance measures of ANN for classification of all kidney stones. Error bars show the standard deviation of performance measures between five folds used in testing.

the data in testing fold is classified. In this classification process, the code also runs until all the data in test folds are classified. When all the stones are classified, it is seen that all of the calcium oxalate and struvite stones are correctly classified while one of cystine stones is also predicted as calcium oxalate. This result is summarized in Table 6.8.

Table 6.8 : Classification results for all stone types.

		Actual Class		
		Calcium Oxalate	Cystine	Struvite
Predicted Class	Calcium Oxalate	35	1	0
	Cystine	0	34	0
	Struvite	0	0	35

2-by-2 confusion matrices are also formed from the information in Table 6.6 in order to analyze performance of this algorithm. Some performance measures, which indicate how successful the algorithm in kidney stone classification is, are calculated making use of the elements of the matrices. The matrices are listed in Table 6.9, 6.10 and 6.11.

Table 6.9 : Confusion matrix for calcium oxalate.

		Actual Class	
		Calcium Oxalate	non-Calcium Oxalate
Predicted Class	Calcium Oxalate	35	1
	non-Calcium Oxalate	0	69

Table 6.10 : Confusion matrix for cystine.

		Actual Class	
		Cystine	non-Cystine
Predicted Class	Cystine	34	0
	non-Cystine	1	70

Table 6.11 : Confusion matrix for struvite.

		Actual Class	
		Struvite	non-Struvite
Predicted Class	Struvite	35	0
	non-Struvite	0	70

The same performance measures, which are accuracy, sensitivity, specificity, precision, recall and F1 score, are also calculated for this algorithm and shown in Table 6.12 and Figure 6.4. As seen from the table and the figure, all performance measures for KNN algorithm are above 99%. These results are excellent and show that the algorithm can successfully categorize the kidney stones from their electromagnetic properties.

Table 6.12 : Performances of KNN for kidney stone classification.

Performance Measures	Calcium Oxalate	Cystine	Struvite	Whole
Accuracy	99.1%	99.1%	100%	99.4%
Sensitivity	100%	97.1%	100%	99.0%
Specificity	98.6%	100%	100%	99.5%
Precision	97.2%	100%	100%	99.1%
Recall	100%	98.6%	100%	99.5%
F1 Score	99.3%	98.1%	100%	99.1%

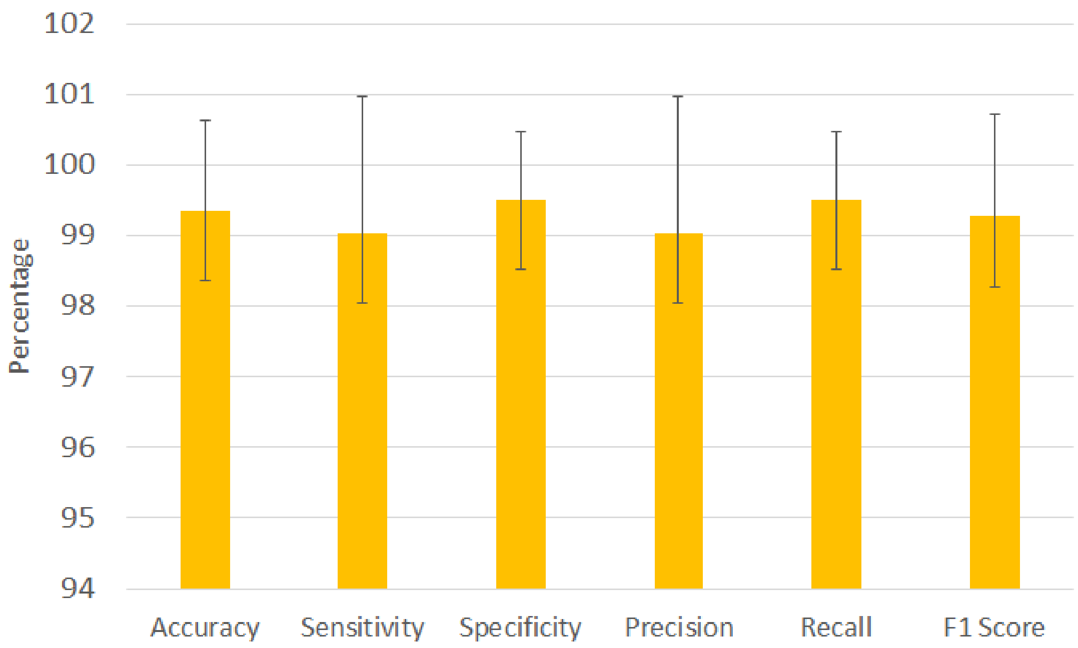

Figure 6.4 : Performance measures of KNN for classification of all kidney stones. Error bars show the standard deviation of performance measures between five folds used in testing.

7. CONCLUSIONS

In this study, kidney stone classification with the help of electromagnetic properties is investigated. Firstly, dielectric property measurements of kidney stones are needed to perform. To this end, taking the measurement frequency range and shape of the material into account, open-ended coaxial line method is preferred. It is assumed that despite this probe is recommended for the use for liquid and semi-solid samples in order to provide direct contact, it is possible to use for kidney stones by being sure that there is no air-gap between the stone and the probe. For this reason, the stones are needed to be sanded before the measurement in order to provide direct contact without any air-gap. After the stones are prepared, the measurements are performed five times for each stone. The measurement frequency is linearly increased from 500 MHz until 6 GHz with 100 MHz steps.

The dielectric constant and dielectric loss factor of each stone are obtained at fifty-six frequency points and then, Cole-Cole fitting is performed to these measured properties. For this purpose, Cole-Cole parameters are required to calculate and GNR method is preferred to find out them. In this method, initial values for all parameters are assigned and they are iteratively updated by using the error which is difference between measured and calculated data. Firstly, it was requested to stop the iteration when the error goes below 0.02. However, calculated parameters for some stones cannot converge to the actual parameters and the error cannot be decreased. To get rid of this problem, initial values are changed for these stone, but it still continues for some of them. In this case, error value is needed to increase to 0.05 and thus, Cole-Cole parameters well-fitting to measurement data can be found for all stones.

Obtained Cole-Cole parameters for 105 kidney stones are fed into two different machine learning algorithms, ANN and KNN. The stones are firstly divided into two groups: training and test. Five folds cross validation is applied in this step and thus, 80% of the data is used to train the algorithm while the remaining is used for test. It can be seen from classification results that this is a good choice for this problem. After grouped the stones, it comes to design the algorithms in which these groups are used.

Firstly, ANN algorithm is designed by selecting layer number, neuron number in each layer, activation functions and training function of the network. Since there is no rule to decide these properties, they are selected with trial and error. The appropriate network architecture for this dataset is determined with this way. As a result, all the performance measures like accuracy, sensitivity and F1-score are calculated above 97% when all stones are classified. Secondly, KNN algorithm is developed by determining the number, k, as 5 and distance measure as Euclidean distance. These properties are also selected with trial and error. In consequence of the classification with this algorithm, the same performance measures are also calculated. They are found above 99% in this time.

In conclusion, methods applied in all steps of this study give successful results and clearly show that type of kidney stones can easily be determined with the help of dielectric properties. More accurate dielectric properties may be obtained with another dielectric property measurement method despite it is tried to be sure about that there is no air-gap resulting in error during measurement. Moreover, in Cole-Cole fitting part, it is seen that GNR highly depends on initial values and it is not a robust method to determine Cole-Cole parameters of kidney stones. Better classification results may also be reached with another numerical method or choosing initial values more accurately. Lastly, since there are a lot of factor determined with trial and error in design of machine learning algorithm, more correct choices that would be improve the performance of algorithms may be made for these factors.

REFERENCES

[1] **Gürbüz, T.U.**, **Aslanyürek, B.**, **Yapar, A.**, **Sahintürk, H. and Akduman, I.** (2014). A Nonlinear Microwave Breast Cancer Imaging Approach Through Realistic Body–Breast Modeling, *IEEE TRANSACTIONS ON ANTENNAS AND PROPAGATION*, *62*(5), 2596–2605.

[2] **Yilmaz, T.**, **Kılıç, M.A.**, **Erdoğan, M.**, **Çayören, M.**, **Tunaoğlu, D.**, **Kurtoğlu, I.**, **Yaslan, Y.**, **Çayören, H.**, **Arkan, A.E.**, **Teksöz, S.**, **Cancan, G.**, **Kepil, N.**, **Erdamar, S.**, **Özcan, M.**, **Akduman, I. and Kalkan, T.** (2016). Machine learning aided diagnosis of hepatic malignancies through in vivo dielectric measurements with microwaves, *Physics in Medicine & Biology*, *61*(13), 5089–5102.

[3] **Fiser, O.**, **Merunka, I. and Vrba, J.** (2016). Waveguide Applicator System for Head and Neck Hyperthermia Treatment, *Journal of Electrical Engineering & Technology*, *11(6)*, 1744–1753.

[4] **Gabriel, S.**, **Lau, R. and Gabriel, C.** (1996). The dielectric properties of biological tissues: III. Parametric models for the dielectric spectrum of tissues, *Physics in Medicine & Biology*, *41*, 2271–2293.

[5] **Rajan, R.**, **Raj, N.**, **Madeswaran, S. and Babu, D.** (2015). Dielectric studies on struvite urinary crystals, a gateway to the new treatment modality for urolithiasis, *Spectrochimica Acta Part A: Molecular and Biomolecular Spectroscopy*, *148*, 266–270.

[6] **Yagyik, Y.**, **Lal, N.**, **Talwar, I. and Jethi, R.** (1989). Electrical conductivity of kidney stones, *Biomaterials*, *10*, 281–285.

[7] **Sinha, D.**, **Anwar, K.**, **Kumari, K.**, **Jaishwal, S.**, **Madeshwaran, S.**, **Keshari, S.**, **Babu, D.**, **Vidya, R. and Nambiraj N, A.** (2012). Studies on the Dielectric properties of Natural Urinary Stones, *Advanced Materials Research*, *584*, 484–488.

[8] **Singh, V.**, **Aganval, R. and Singh, V.** (1991). Piezoelectric Effect in Renal Calculi, *lEEE TRANSACTIONS ON BIOMEDICAL ENGINEERING*, *38*(2), 218–219.

[9] **Kumarpranawa, I.K.**, **Saranya, D. and Raj, A.** (2015). Preparation and Characterization of Kidney Stone Phantoms with Compression Strength and Dielectric Property Studies, *International Journal of ChemTech Research*, *8*(5), 153–157.

[10] **Singh, V.**, **Lafaut, J.**, **Weversa, M.**, **Vincent, C. and Baed, L.** (1999). Stress-Generated Potential in Renal Calculi and Lithotripsy, Proceedings of The First Joint BMES/EMBS conference.

[11] **Abdulsalim, M.** (2012). The characteristics, dielectric properties and surface morphology of calcium oxalate monohydrate single crystals grown in silica gel, *Journal of Chemical, Biological and Physical Sciences*, *2*(2), 962–967.

[12] **Paul, I.**, **Varghese, G.**, **Ittyachen, M.A.**, **Mathew, K.T.**, **Lonappan, A.**, **Jacob, J. and Kumar, S.** (2002). Dielectric Properties of Urinary Stones at Microwave Frequencies, *MICROWAVE AND OPTICAL TECHNOLOGY LETTERS*, *35*(4), 297–299.

[13] **Serrat, J.**, **Lumbreras, F.**, **Blanco, F.**, **Valiente, M. and López-Mesas, M.** (2017). myStone: A system for automatic kidney stone classification, *Expert Systems With Applications*, *89*, 41–51.

[14] **Viswanath, K.**, **Gunasundari, R. and Hussan, S.** (2015). VLSI Implementation and Analysis of Kidney Stone Detection by Level Set Segmentation and ANN Classification, *Procedia Computer Science*, *48*, 612–622.

[15] National Cancer Institute SEER Training Modules - Urinary System, `https://training.seer.cancer.gov/anatomy/urinary/components/`, accessed on 04/02/2018.

[16] National Institute of Diabetes and Digestive and Kidney Diseases - Urinary Diseases, `https://www.niddk.nih.gov/health-information/urologic-diseases`, accessed on 04/02/2018.

[17] **Romero, V.**, **Akpinar, H. and Assimos, D...e.** (2010). Kidney stones: a global picture of prevalence, incidence, and associated risk factors, *Reviews in urology*, *12(2-3)*(2/3), e86–e96.

[18] Medical Park Hospital - Patient Guide about Kidney Stones, `http://www.bobrektasitedavisi.net/bobrek-taslari/`, accessed on 18/02/2018.

[19] **Andreassen, K.**, **Poulsen, A.**, **Olsen, P.**, **Aabeck, J. and Osther, P.** (2007). Classification of urolithiasis in Denmark: a national survey, *European Urology*, *2*(1), 126.

[20] How do kidney stones form?, `http://www.kidneystoners.org/information/how-do-stones-form/`, accessed on 08/02/2018.

[21] **Schulsinger, D.A.** (2015). *Kidney Stone Disease*, Springer International Publishing.

[22] **Basiri, A.**, **Taheri, M. and Taheri, F.** (2012). What is the State of the Stone Analysis Techniques in Urolithiasis?, *Urology Journal*, *9*(2), 445–454.

[23] **Semenov, S.Y.**, **Posukh, V.G.**, **Bulyshev, A.E.**, **Williams, T.C.**, **Sizov, Y.E.**, **Repin, P.N.**, **Souvorov, A. and Nazarov, A.** (2006). Microwave Tomographic Imaging of the Heart in Intact Swine, *Journal of Electromagnetic Waves and Applications*, *20*(7), 873–890, `https://doi.org/10.1163/156939306776149897`, `https://doi.org/10.1163/156939306776149897`.

[24] **Kremer, F. and Schönhals, A.** (2003). *Broadband Dielectric Spectroscopy*, Springer-Verlag Berlin Heidelberg.

[25] **Campbell, A.M.** (1990). Measurements and Analysis of the Microwave Dielectric Properties of Tissues, *Ph.D. thesis*, University of Glasgow.

[26] Keysight Technologies, "Basics of Measuring the Dielectric Properties of Materials ", `http://literature.cdn.keysight.com/litweb/pdf/5989-2589EN.pdf`, accessed on 13/03/2018.

[27] **MISRA, D.** (1987). A Quasi-Static Analysis of Open-Ended Coaxial Lines, *IEEE TRANSACTIONS ON MICROWAVE THEORY AND TECHNIQUES*, *MIT-35*(10), 925–928.

[28] **Alpaydın, E.** (2014). *Introduction to Machine Learning*, Massachusetts Institute of Technology Press.

[29] **Russell, S. and Norvig, P.** (2010). *Artificial Intelligence: A Modern Approach*, Prentice Hall.

[30] Keysight N1501A Dielectric Probe Kit, `https://literature.cdn.keysight.com/litweb/pdf/5992-0264EN.pdf?id=2605692`, accessed on 17/03/2018.

[31] **Kiourti, A.**, **Sun, M.**, **He, X. and Volakis, J.** (2014). Microwave Cavity with Controllable Temperature for In Vitro Hyperthermia Investigations, *JOURNAL OF ELECTROMAGNETIC ENGINEERING AND SCIENCE*, *14*(3), 267–272.

[32] **Jusoh, A.**, **Abbas, Z.**, **Hassan, J. and Fahad, A.** (2011). A Simple Procedure to Determine Complex Permittivity of Moist Materials Using Standard Commercial Coaxial Sensor, *MEASUREMENT SCIENCE*, *11*(1), 19–22.

CURRICULUM VITAE

Name Surname: Banu SAÇLI

Place and Date of Birth: Şişli / 28.05.1992

E-Mail: banusacli@gmail.com

EDUCATION:

- **B.Sc.:** 2015, Yeditepe University, Faculty of Engineering and Architecture, Department of Biomedical Engineering

PROFESSIONAL EXPERIENCE AND REWARDS:

- 2017 Research Assistant at Istanbul Technical University.
- 2016-2017 Research Assistant at Erzincan University.
- 2015-2016 Biomedical Specialist at Medicalpark Bahçelievler Hospital

PUBLICATIONS, PRESENTATIONS AND PATENTS ON THE THESIS:

- Önal, E.G., Keleşsoğlu, A., Saçlı, B., Cansız, G., Joof, S., Aydınalp, C. and Çayören, M., 2017. Kidney Stone Classification with Electromagnetic Properties: Preliminary Results. *International Congress - Telecominications Forum Conference*, November 21-22, 2007 Belgrade, Serbia,